



Carlos Albarracín Mitjavila

Design and Optimization of a Microstereolithography 3D-Printer

Master's thesis, which has been submitted for verification of professional development for the degree of Master of Science in Technology.

Espoo, 29.5.2017

Thesis Supervisor: Prof. Jouni Partanen

Thesis Advisor: Eero Huutilainen

Author Carlos Albarracín Mitjavila		
Title of thesis Design and Optimization of a Microstereolithography 3D Printer		
Degree programme MSc Mechanical Engineering		
Major/minor Mechanical Engineering	Code Exchange Student	
Thesis supervisor Professor Jouni Partanen		
Thesis advisor(s) Eero Huutilainen		
Date 29.5.2017	Number of pages 56	Language English

Abstract

Stereolithography is a rapid prototyping technology with a hundred-micron-scale resolution based on the process of curing a photopolymer by the interaction of one photon of light with a photoinitiator and/or a photosensitizer. It is a surface based technique where the structure is constructed layer-by-layer. In *Mask image Projection* approach, the entire cross section is cured by using a Dynamic Mask Generator.

The aim of this thesis was the construction of a Mask Projection Microstereolithography (MP μ SL) 3D printer, whose operation is similar to the one mentioned before, but its goal is to print samples with a 5 μ m resolution. A Digital Micromirror Device (DMD) from a commercial projector was used as Dynamic Pattern Generator, the one will create the desired image on the resin once the UV light from a LED has polymerized it. Moreover, an elevator device, formed by a stepper motor and a linear guide, was used to enable the spread of fresh resin on the top of the already polymerized layer, so it is possible to start the light-induced solidification process of the next.

Once the machine was built, produced samples were analyzed with an electronic (SEM) and an optic microscope to optimize its functioning. With those analysis, it was possible to measure the horizontal resolution of the 3D-printer (4.41 μ m²), while corroborating its correct operation.

One of the most important lines of work would be the development of a device that allows a precise measurement of the distance between the platform and the resin vat, since at this moment this process is done intuitively and in case of using resins with a low depth of penetration, it is a very complicated task

Keywords Additive Manufacturing, Rapid Prototyping, Photopolymer, Stereolithography, Mask Projection Microstereolithography

Preface

First of all, I would like to thank Dr. Jouni Partanen and doctoral candidate Eero Huottilainen for their help throughout this long process, from the choice of the topic to the final drafting of the report. Thank you for trusting me and letting me be part of this project.

In addition, I would like to thank all the support received by doctoral candidates, Pekka Lehtinen and Tuukka Verho, both with an extensive knowledge on the subject. Thank you for your patience, your advice, and your encouragement, which have helped me to finish the thesis in a way that is more than satisfactory.

I would also like to thank all the members of the AddLab, especially to Mr Francés Segura González and doctoral candidates Meng Wang and Ashish Mohite, for making me feel part of the team, creating a more than suitable environment in which to work, and helping me at any time.

Finally, I would like to thank my father, mother, brother and sister. For supporting me in every single step along this long process, and for making me believe I can achieve any goal.

Espoo, 29.5.2017

Carlos Albarracín Mitjavila

Carlos Albarracín Mitjavila

Table of contents

Abstract	ii
Preface	iii
Table of contents	iv
Labeling of variables used	viii
Abbreviations	ix
1 Introduction	1
1.1 Background	1
1.2 Research objective	3
2 Stereolithography	4
2.1 Introduction	4
2.2 Photopolymers	4
2.2.1 Introduction	4
2.2.2 Photopolymerization	5
2.2.3 Photocrosslinking	6
2.3 Resolution	6
2.3.1 Vertical resolution	6
2.3.2 Lateral resolution	8
3 Microstereolithography	9
3.1 Introduction	9
3.2 Different techniques	9
3.2.1 Vector scan	9
3.2.2 Mask projection	10
3.2.3 Two photon polymerization	12
3.3 Existing projection microstereolithography systems	13
3.3.1 Liquid crystal display (LCD) based projection microstereolithography	13
3.3.2 Spatial light modulator (SLM) based projection microstereolithography	14
3.3.3 Digital mirror device (DMD) based projection microstereolithography	15
3.3.4 Liquid Crystal on Silicone (LCoS) based projection microstereolithography	16
4 Equipment and materials	17
4.1 Introduction	17
4.2 Light source	18
4.3 Digital micromirror device	19
4.4 Optical components	20
4.5 Resin vat	22
4.6 Platform	22
4.7 Elevator device	23
4.8 Electronic components and software	24
4.9 Resins	28
4.10 Electronic Microscope	30
5 Final set up	33
6 Experiments and results	35
7 Summary and conclusions	42
References	44
Appendix	

Table 1. LCD based projection microstereolithography systems [7]	13
Table 2. based projection microstereolithography systems [7].....	15
Table 3. Different solutions for each one of the components of the MPμSL system [7].....	18
Table 4. HTMV2's machanical properties	28
Table 5. PDMS's properties	29
Table 6. Differences between Scanning Electron and Transmission Electron Microscopes	32
Table 7. Master's Thesis budget	1
Figure 1. Schematic of a Mask Projection Microstereolithography 3D-Printer [7]	2
Figure 2. Different orientations in the stereolithography technique [12]	4
Figure 3. Molecular structure of different polymers [13]	5
Figure 4. Relationship between the thickness of the polymerized layer and (a) photoinitiator and (b) neutral absorbers concentration [11]	7
Figure 5. Relationship between the width of the polymerized layer and (a) the photoinitiator and (b) the neutral absorber concentration [11]	8
Figure 6. Schematic of vector scan procedure, based on the scanning of a focused light beam on the surface of a photosensitive resin [17].....	10
Figure 7. (a) Constrained and (b) free surface techniques [5].....	10
Figure 8. Schematic of mask projection procedure, where a Dynamic Pattern Generator produces the image to print [17].....	11
Figure 9. Schematic of top-down orientation approach. As shown, the Z-stage descends and the light is projected from above [18]	11
Figure 10. Schematic of bottom-up orientation approach, where the Z-stage moves upwards and the light is projected from below [18]	12
Figure 11. Two-photon process. Two photons reach the transition energy between the excited and the ground state	13
Figure 12. Schematic of SLM based projection microstereolithography. The final printed image will depend on the state of the SLM in every single moment [19]	14
Figure 13. Scanning-electron microscopy photograph of the microgear printed using a SLM as a Dynamic Pattern Generator [19]	14

Figure 14. Micromirror from a DMD. The final image will depend on the state of all of the micromirrors that are part of the DMD	15
Figure 15. Schematic of the performance of this Liquid Crystal on Silicone devices [22]	16
Figure 16. Set-up of a Mask Projection Microstereolithography 3D-printer	17
Figure 17. LED selected as light source (410 nm)	18
Figure 18. RCD connections. 1: LED wires, 2: Arduino wire, 3: power source and 4: resistors	19
Figure 19. Schematic of DMD. Depending on its position, the light will bounce and will be directed to polymerize the photopolymer, or on the contrary, will be diverted [24]	20
Figure 20. DMD used. The red arrows show the path followed by the light that will polymerize the photopolymer, this is, the light bounced by the micromirros in active mode	20
Figure 21. Divergent light. Theses lenses avoid light's divergence, i.e., keep it parallel [25] ..	21
Figure 22. AL3026-A - Ø30 mm aspheric lens. Manufacturer: Thorlabs [26]	21
Figure 23. 75mm focal length lens.....	21
Figure 24. N10X-PF - 10X Nikon Plan Fluorite Imaging Objective. Manufacturer: thorlabs [27]	22
Figure 25. Platform used. Device to which the first layer is attached to.....	22
Figure 26. a) linear guide (Movetec: KK4001P-100A1) [28] and b) stepper motor (Movetec: PK244PDA-P10-L) [29].....	23
Figure 27. Coupling between stepper motor and linear guide. This device transmits the motor's movement to the linear guide.....	24
Figure 28. Electronic parts of the 3D printer. (1) Arduino 1, (2) Arduino 1, and (3) projector.	24
Figure 29. Arduino-Mega attached to RAMPS 1.4. This device will control the LED and the stepper motor to get a perfect synchronization between them.....	25
Figure 30. Creation Workshop's interface.....	26
Figure 31. Configure menu	27
Figure 32. Slices 100 (left) and 179 (right).....	27
Figure 33. Python's software interface	28
Figure 34. Resin vat with a thick layer of PDMS.....	29
Figure 35. Part that can not be manufactured by conventional processes [32]	30

Figure 36. Schematic of the CLIP process. The permeable window creates a dead zone where the polymerization cannot occur [33]	30
Figure 37. TEM's schematic. The electrons pass through the sample generating a pattern in the fluorescent screen [36]	31
Figure 38. SEM's schematic. The electron beam scans the sample's surface [37]	32
Figure 39. (1) stepper motor, (2) platform, (3) linear guide, (4) microscope objective, (5) mirror, (6) led with aspheric lens, and (7) DMD	33
Figure 40. Path followed by the beam of light	34
Figure 41. Projected and desired projected image	34
Figure 42. Draw used to determine the vertical resolution	35
Figure 43. Olympus microscope BH-2	35
Figure 44. Patron obtained to calculate horizontal resolution	36
Figure 45. Problems on the horizontal resolution (from the left to the right: a, b and c)	36
Figure 46. Printed square	37
Figure 47. Damaged sample due to the SEM microscope	37
Figure 48. Thickness of a sample	38
Figure 49. 10 μ m sample thickness.....	38
Figure 50. 100 μ m sample thickness.....	39
Figure 51. Combination of different cross section areas	39
Figure 52. Analysis of the thickness. Three layers of 20 μ m each	40
Figure 53. 4-layer sample	40
Figure 54. Analysis of the thickness. Four layers of 20 μ m each	41
Figure 55. Different geometries	41

Labeling of variables used

c	$\frac{mol}{L}$	Photoinitiator concentration in the resin
e	μm	Polymerized layer thickness
F_0	$\frac{photons}{m^3 s}$	The light flux reaching the surface of the resin
L	μm	Width of the polymerized layer
T	$\frac{Photons}{m^3}$	Irradiation threshold
t	s	Irradiation time
t_0	s	Threshold irradiation time required to initiate a reaction
α	$\frac{L}{mol} m$	Napierian coefficient of molar extinction for the photoinitiator

Abbreviations

2D	Two Dimensional
3D	Three Dimensional
μ SL	Microstereolithography
AM	Additive Manufacturing
CAD	Computer Aided Design
DMD	Digital Micro-mirror Device
GUI	Graphical User Interface
HDMI	High Definition Multimedia Interface
h ν	Light
LCD	Liquid Crystal Display
LCoS	Liquid Cristal on Silicone
LED	Light-emitting Diode
LOC	Lab On a Chip
MP μ SL	Mask Projection Microstereolithography
PI	Photoinitiator
PI*	Excited Photoinitiator
PD	Photosensitizer
P μ SL	Projection Microstereolithography
RP	Rapid Prototyping
R*	Radical
R+	Cation
SL	Stereolithography
STL	Triangular mesh model format
UV	Ultraviolet

1 Introduction

1.1 Background

Rapid prototyping (RP) is a process used to manufacture plastic, metal or even ceramic. As its name indicates, the purpose of this technique is to create prototypes of a particular model in order to facilitate the work of the operators in charge of the development of a particular product.

Users of this technique have realized that this term is currently inadequate due to the development that it has experienced in the last years. Nowadays almost any geometry can be manufactured, i.e., there is a much closer link to the final product, so many parts are in fact directly manufactured in these machines [1]. This is the reason why a new term was adopted, Additive Manufacturing, although RP is still used [1].

As in RP, AM manufactures the desired product based on a three-dimensional Computer Aided Design (3D CAD) model. Although different techniques might be used, most of the processes involve, in one way or another, the following seven steps [1]:

1. Design of the model (3D CAD)
2. Conversion to STL style format, this is, the CAD model is transformed into a triangular polygon mesh
3. Slice and transfer the STL file to the AM machine
4. Machine Setup such as curing time, layer thickness, material used, etc.
5. Printing the object
6. Post processing might be required in certain applications, for example, when supporting features have been manufactured
7. Use the product for the application for which it was built

Different materials can be used depending on the AM machine. Liquid polymers are used for Stereolithography (SL), a rapid prototyping technology with a $150\mu\text{m}$ resolution patented in 1984 [2] [3].

Two different approaches exist on the stereolithography technology. The first one, based on the initiation of curing a resin by the interaction of one photon of light with a photoinitiator (PI) and/or a photosensitizer (PS). It is a surface based technique where the structure is constructed layer-by-layer [4], i.e., the product is not built inside the resin but on its surface. And the second one, where the structure is created directly in the resin (two-photon polymerization).

Within the first approach, either Vector Scan or Mask Projection techniques can be used. In the Vector scan, a laser beam is focused and scanned on the open surface of the photosensitive liquid, occurring a local transformation due to the presence of a photoinitiator, which allows to create a certain layer of the desired object. When a layer is finished, fresh resin is spread on top of the already manufactured part of the object, and the light-induced solidification of the next layer is started [5]. On the other hand, in the Mask Image Projection approach, the entire cross section is cured by using a dynamic mask generator (Liquid Crystal Display (LCD), Digital Mirror Device (DMD), or Liquid Crystal on Silicone (LCoS)). The slow development of this latter method was due to

the late commercial availability of the components required for the dynamic pattern-generator (1995) [5].

Due to the development of nanomanufacturing, new 3D printing techniques have emerged in order to offer a solution to the problem associated to its manufacture [6]. Microstereolithography, a technique based on the principle used in stereolithography, with development started in 1993 [5], is the method used for the manufacture of these nanoproducts.

In 1995 Arnaud Bertsch presented the first Mask Projection Microstereolithography (*MP μ SL*) [7], which is the 3D printer to be studied in this Master's thesis and whose schematic can be observed in Figure 1:

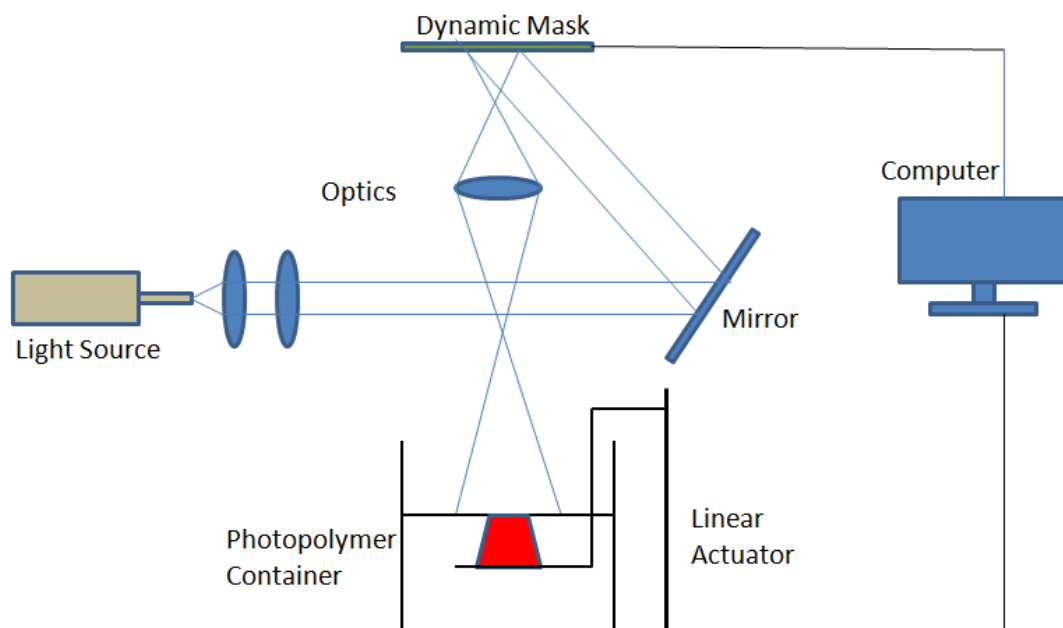


Figure 1. Schematic of a Mask Projection Microstereolithography 3D-Printer [7]

MicroTec, based in Duisborg, Germany, was the first company to sell components for rapid prototyping applications, the first commercial application for microstereolithography [8]. Nevertheless, nowadays there are many other applications for the products manufactured with this technique, such as objects with complex geometry, small mechanical components, microfluidic components and Microsystems components.[5]

In the medical field, some advances have been achieved due to this technique, such as a method for applying microstereolithography in the construction of 3-D cartilage scaffolds [9] [4]. Moreover, Jan Tøpholm, Søren Westermann, and Svend Vitting Andersen created a technique based on stereolithography 3D printing to create a patient-specifically customized hearing aid: in order to create a mold of the patient's ear canal, some liquid silicone is injected inside their ear. Once solidified, the mold is converted into a 3D model and imported into a CAD software. Then it is converted into a STL file and sent to a 3D printer (stereolithography) for manufacturing. Once the hearing aids have been printed, the micro-circuitry that processes and amplifies sound is packed into the custom shell [10].

As mentioned before, microstereolithography has to be understood as a potential manufacturing technique in certain cases, and not as a mere prototyping method. That is because it enables manufacturing of parts that cannot be produced by conventional manufacturing methods. Finally, extensive research is being made on the use of composite materials with this technique, further facilitating its use as a direct manufacturing method.

The expansion of this technique would be a revolution, especially in the case of Lab On a Chip (LOC), thanks to which, in developing countries, you can have effective diagnostics in minutes. It will be possible to diagnose millions of people with budgets much tighter than they are today. If LOCs prove to be reliable for several months under extreme conditions of temperature and humidity, always maintaining an affordable price, millions of lives could be saved thanks to more accurate and early diagnostics.

1.2 Research objective

The objective of the thesis is to build a Mask Projection Microstereolithography 3D printer in order to be able to obtain objects of the order of magnitude of micrometers. As a source of light, a UV LED is going to be used to polymerize a photopolymer. To obtain the desired sample with good quality, two aspheric lenses will be needed to collimate the beam of light, while the 2D pattern that will be polymerized, is produced by a digital micromirror device (DMD), obtained from a commercial projector.

Once built, the objective will be to iteratively optimize its operation, that is, to try to adjust the necessary parameters in order to obtain samples of the highest possible quality, this is, neither fuzzy nor deformed. To achieve this goal, it will be necessary to determine the focal length of each of the lenses and the working distance of the microscope, to obtain an image as focused as possible. It will also be necessary to determine the optimum curing time for the resin to be used.

In addition, we will determine the horizontal resolution of the machine built, i.e., the area that represents each pixel of the DMD in the final piece. Finally, we will try to print simple pieces in order to verify the correct operation of the whole system.

2 Stereolithography

2.1 Introduction

Stereolithography was the first modern additive manufacturing technique process. It utilizes ultraviolet light for curing photopolymeric resin in a tank. By that curing process it is possible to create objects layer-by-layer, each layer being a cross section of the desired object. The term stereolithography was chosen by Charles W. Hull, when he patented the process in 1986 [11].

The UV light, which can be emitted from a LED, a laser or a lamp, cures the resin layer-by-layer. Once a layer is cured, the platform to which the item is attached, scrolls vertically, depending on the on the orientation selected, Figure 2, to cure a new layer over the previous one (the different orientations will be explained later on).

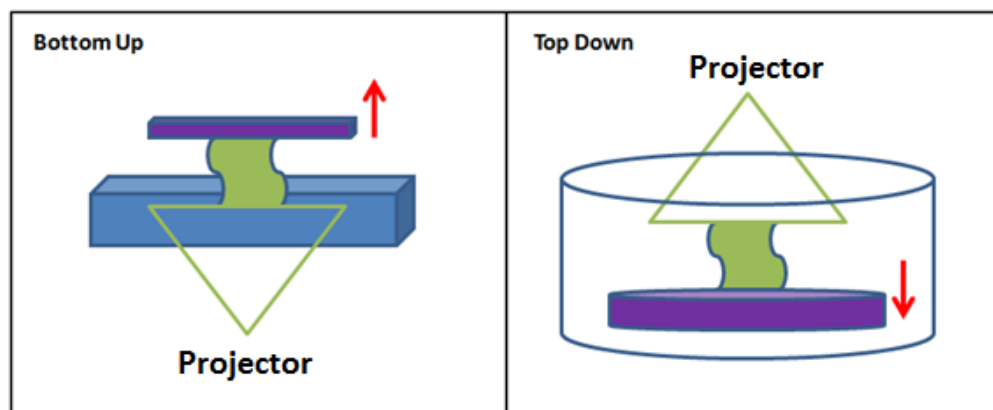


Figure 2. Different orientations in the stereolithography technique [12]

These kind of 3D printers can create complex objects, some of which are impossible to manufacture with conventional methods. That is the reason why several industries — from medical to manufacturing — use stereolithography not only to build prototypes, but also to build final products. On the other hand, there are certain industries, for example automotive industry, which cannot use SL for building the final product, but they might use stereolithography to create a prototype casting of a car door handle in order to test it for fit and form and, once perfected, can serve as the master pattern for a machined auto part [13].

2.2 Photopolymers

2.2.1 Introduction

Resins used in microstereolithography 3D printers are characterized for the presence of monomers, oligomers (which consist of few monomers) and photoinitiators. Photoinitiators are in charge of the absorption of the light in order to start the polymerization process, i.e., they convert the light into chemical energy. It is also possible to add neutral absorbers into those resins in order to reduce the layer thickness of the desired object. This thickness reduction is possible because of the absorption and dissipation of the light that these neutral absorbers produce.

Moreover, depending on the molecular structure of the polymers, they might be able to melt and solidify repeatedly. While some polymers present linear or branched structure, as shown in Figure 3, the polymers used in SL present a cross-linked one. This structure allows them not to melt and exhibit much less creep break and stress relaxation [1].

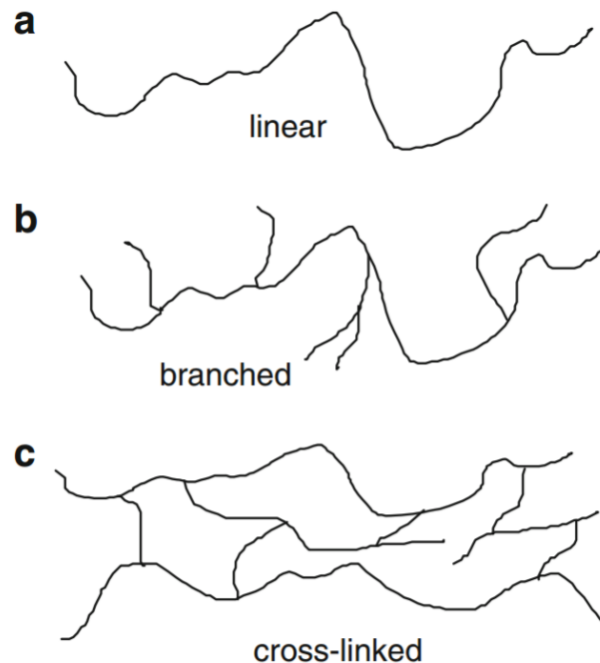


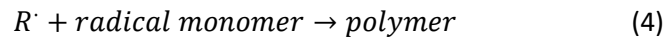
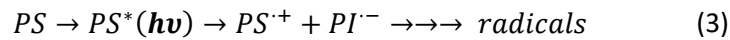
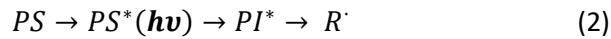
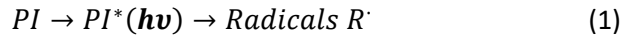
Figure 3. Molecular structure of different polymers [13]

Patents of acrylate and epoxide resins appeared around 1990 [1]. On the one hand, in acrylates, some extra-curing can take place, increasing the stresses in those areas, which could cause the damage of the desired object. On the other hand, epoxide composition for SL resins leads to a lower level of shrinkage. Moreover, they are not inhibited by atmospheric oxygen. However, they decrease the speed and increase the brittleness of the material. That is the reason why the resins most commonly used for SL are epoxides with some acrylate content [1] in order to combine advantages of both of them, while trying to minimize their drawbacks.

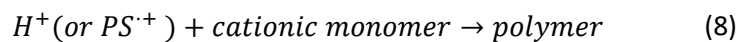
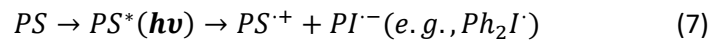
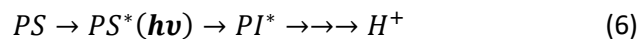
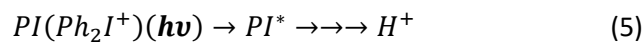
2.2.2 Photopolymerization

Polymerization is the process by which reacting monomer molecules come together to form polymers. In the photopolymerization, the energy necessary to form those polymers comes from the absorption of visible or ultraviolet light. There are three different types of photopolymerization: free radical photopolymerization (which takes place in acrylate resins), cationic polymerization (which takes place on epoxy resins) and free radical promoted cationic polymerization.

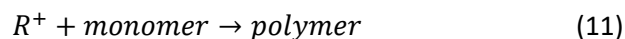
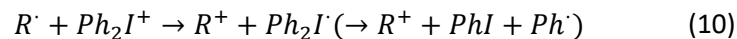
A free radical photopolymerization can only take place if a photoinitiator (PI) and/or a photosensitizer (PS) are present in the resin in order to absorb the light. PI becomes excited (PI^*) with certain light generating a radical R^* (1). Those radicals can also be formed from the PS, where the PS excited has to move from its state to PI by energy (2) or electron transfer (3) [14]:



In cationic polymerization, onium salts are used as PI. Their homolytic/heterolytic decomposition followed by hydrogen transfer reactions leads to a proton. Their photosensitized decompositions occur according to energy (6) or electron transfer (7) [14]:



Finally, in free radical promoted cationic polymerization (FRPCP) (9–11), a radical, R^\cdot , is produced from a radical source (RS) (a PI or a PS can play such a role) and then oxidized by Ph_2I^+ to form Ph_2I^\cdot and a cation, R^+ , suitable for the ring opening reaction (ROP) of epoxides or the cationic polymerization of vinyl ethers (the Ph_2I^\cdot species readily decomposes into PhI and Ph^\cdot : [14])



2.2.3 Photocrosslinking

Photocrosslinking describes the process of formation of covalent bonds between oligomers by opening double bonds. The main difference between this process and photopolymerization is that the latter one is only light dependent on the first step, while photocrosslinking is light dependent in every single step.

2.3 Resolution

2.3.1 Vertical resolution

Vertical resolution depends directly on the thickness of the polymerized layers. It is important to highlight that the layer thickness does not depend on the thickness of fresh

resin prepared to be polymerized, but on the penetration depth inside the liquid photopolymer resin. After a lot of research within this topic [15] [16], an equation that shows the evolution of the thickness of the cured layer with irradiation has been found:

$$e = \frac{1}{\alpha c} \ln\left(\frac{t}{t_0}\right), \text{ with } t = \frac{T}{\alpha c F_0} \quad (12)$$

Where:

- e = polymerized layer thickness (μm)
- α = napierian coefficient of molar extinction for the photoinitiator ($\frac{\text{L}}{\text{mol m}}$)
- c = photoinitiator concentration in the resin ($\frac{\text{mol}}{\text{L}}$)
- t_0 = threshold irradiation time required to begin the reaction (s)
- t = irradiation time
- T = irradiation threshold value ($\frac{\text{Photons}}{\text{m}^3}$)
- F_0 = the light flux reaching the surface of the resin ($\frac{\text{photons}}{\text{m}^2 \text{s}}$)

As it is shown in equation 12, two different approaches can be made in order to decrease the layer thickness. Either decrease the irradiation time (t) or increase the amount of Photoinitiators (c) or neutral absorbers. Both of the mentioned solutions are suitable for this purpose.

Although at first glance it might seem that reducing the irradiation time for one slightly higher than the threshold irradiation time has no drawbacks, it can be observed that any small change in irradiation will strongly affect the layer thickness, the one will become really difficult to control, which is, however, the opposite that was intended to be achieved. That is the reason why it is necessary to take a very precise control during the curing process if this is the chosen method to improve vertical resolution.

If the second approach is the one that is going to be chosen, it is important to remark that the addition of neutral absorbers might reduce considerably the resin's reactivity, which leads to an increase in the curing time. Nevertheless, Figure 4 shows the influence on the layer thickness when increasing the amount of these components on the resin:

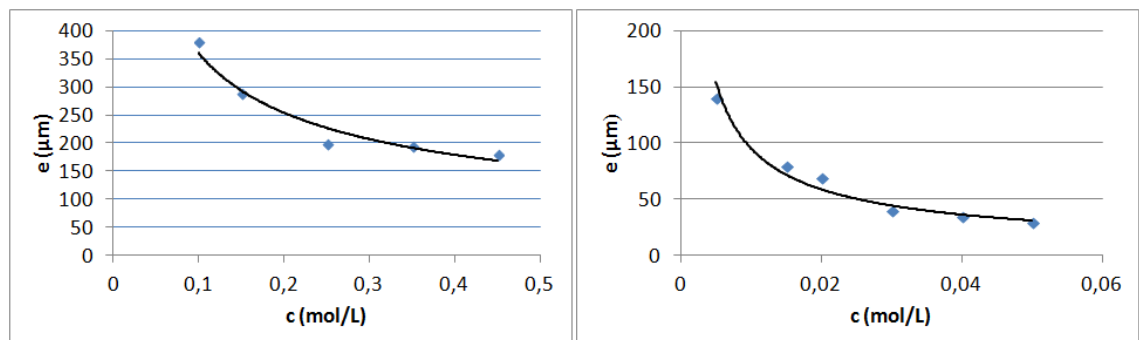


Figure 4. Relationship between the thickness of the polymerized layer and (a) photoinitiator and (b) neutral absorbers concentration [11]

It is shown how the increase on the concentration of (a) photoinitiators or (b) neutral absorbers, decreases the thickness of the polymerized layer, i.e., the vertical resolution improves considerably.

It is important to have into consideration that an adequate proportion of neutral absorbers and photoinitiators must be present in the resin in order to obtain the desirable conditions for photopolymerization reaction, this is, strong reactivity and strong absorption. If this proportion previously mentioned is not present in the resin, undesirable consequences will appear, such as, lack of polymerization, thick polymerized layers or unwanted polymerization [11].

2.3.2 Lateral resolution

Lateral resolution strongly depends on the stereolithography method used. In the mask projection approach, lateral resolution depends on the optics used. Moreover, a microscope objective is normally used in order to decrease the spot size of the focused light beam, increasing therefore, the lateral resolution. If on the contrary, scan mask approach is to be used, lateral resolution will depend on the laser beam diameter as much as on the laser beam system's accuracy. Lateral resolution can also be improved by using low viscosity resins (which flow better) and adjusting the right curing time for each specific resin.

The processes previously mentioned to increase vertical resolution also slightly affect lateral resolution, as is shown in Figure 5:

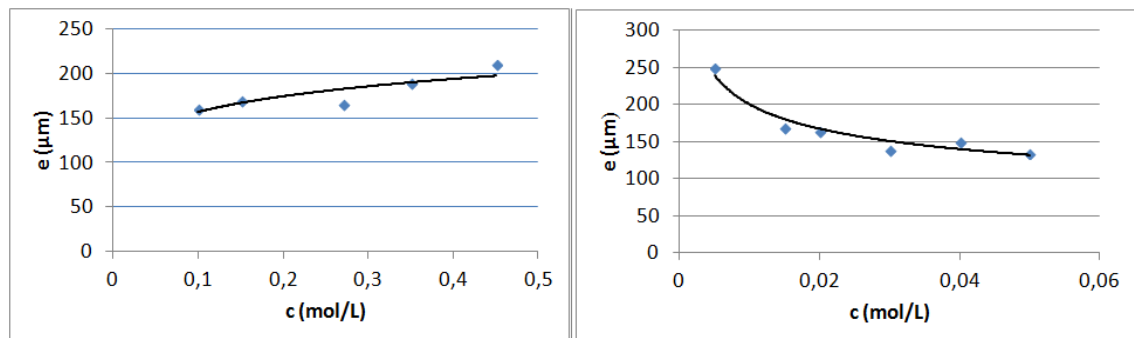


Figure 5. Relationship between the width of the polymerized layer and (a) the photoinitiator and (b) the neutral absorber concentration [11]

Figure 5.a) shows the evolution of the width (l) with photoinitiator concentration. It can be inferred how the addition of photoinitiators produces an increase on the width of the polymerized layer, which leads to a decrease on the lateral resolution. On the other hand, Figure 5.b) shows a decrease on the width of the polymerized layer when increasing neutral absorbers concentration, which yields to an increase on the lateral resolution. Nevertheless, as mentioned before, the addition of neutral absorbers will increase curing time due to the loss of the resin reactivity, which leads to a reduction of the production speed.

3 Microstereolithography

3.1 Introduction

As mentioned before, a great advancement of micro electro-mechanical systems (MEMS) technology has been observed in the last years. The manufacture of three-dimensional structures will provide new microfluidic capability that is challenging, if not impossible, to make with existing approaches. Microstereolithography, a technique based on SL, is trying to solve some of the problems generated while manufacturing the products previously mentioned.

As SL, it is based on the polymerization of a photopolymeric resin in order to manufacture the desired object layer-by-layer. The biggest advantage of this technique is the possibility to manufacture objects with $5\mu\text{m}^2$ horizontal resolution. Different approaches and techniques within microstereolithography will be explained in this section in order to get the whole picture.

Some of the terms that will be used henceforth are defined as follows:

- Layer thickness (μm): value that represents the thickness of each layer
- Minimum feature size (μm): defines the lateral resolution
- Vertical build rate (mm/s): defines the process speed. It is very difficult to compare this term between different published works due to varying terminology.

3.2 Different techniques

As mentioned before, there are different techniques or approaches within the stereolithography 3D printing that were categorized by Gibson et al. [1]:

- Vector scan
- Mask projection
- Two-photon irradiation

3.2.1 Vector scan

In this process, each layer is made by scanning a focused light beam on the surface of a photosensitive resin. Once a layer is built, the platform scrolls down so a new layer can be polymerized over the previous one. The precision of this technique will depend mostly on the radius of the light beam, which depends on how precisely the beam is focused. A schematic of this procedure is shown in figure 6:

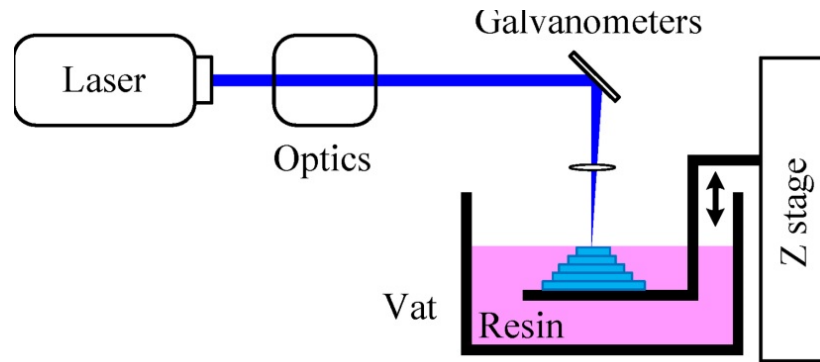


Figure 6. Schematic of vector scan procedure, based on the scanning of a focused light beam on the surface of a photosensitive resin [17]

Within this procedure, the two main approaches that have been built are the ones shown in Figure 7:

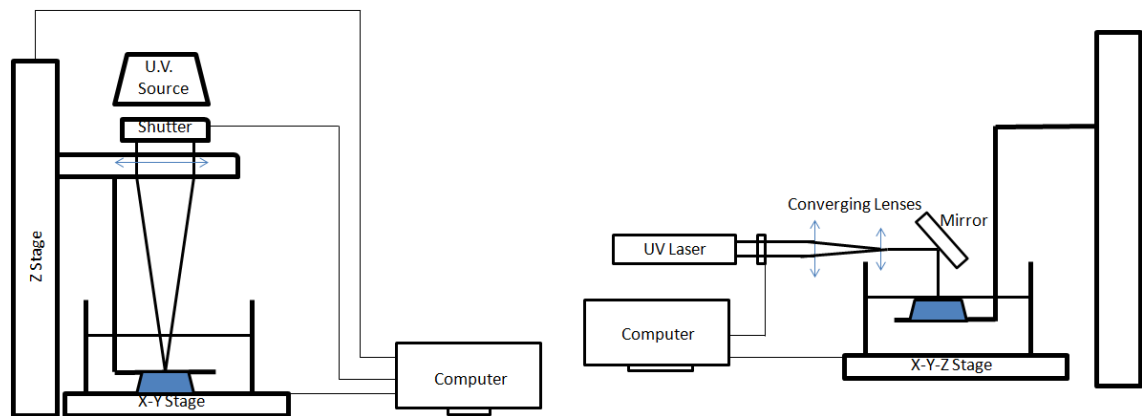


Figure 7. (a) Constrained and (b) free surface techniques [5]

While Figure 7a. presents a glass window on the resin's surface in order to obtain a layer of constant thickness, Zissi et al. described the one shown in Figure 7b., called "*free surface technique*" to avoid the adhesion of the polymer to the transparent window [5].

3.2.2 Mask projection

As mentioned before, this technique experienced a late development due to the lack of commercially available dynamic pattern generators, which are the differentiating component of this method. Unlike vector scan, every layer is made in one irradiation step. In this case, the shape of the layer will depend on the Dynamic Pattern Generator, i.e., there will be a source of light pointing to this pattern generator, the one, depending on its configuration, will only allow some of it to get to the resin and polymerize it. A schematic of this method is shown in Figure 8, where a DMD acts as the Dynamic Pattern Generator:

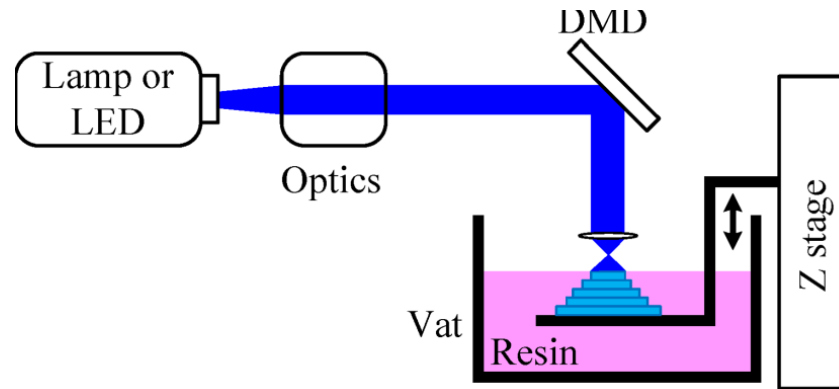


Figure 8. Schematic of mask projection procedure, where a Dynamic Pattern Generator produces the image to print [17]

Depending on the relative position between the light source and the resin vat there are different approaches within this technique: top-down, bottom-up and side-wise orientation approaches.

3.2.2.1 Top down orientation approach

As a mask projection method, each section is polymerized at once with the help of a Dynamic Pattern Generator, as seen in Figure 9:

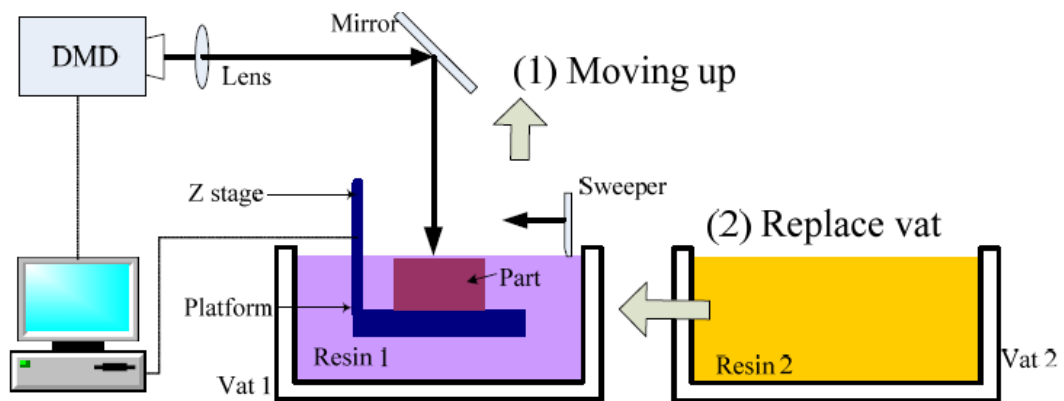


Figure 9. Schematic of top-down orientation approach. As shown, the Z-stage descends and the light is projected from above [18]

The main feature of this method is the movement of the platform once a layer has been polymerized. As the image is projected from above, once a layer is polymerized, the platform descends, leaving a new layer of fresh resin that will be polymerized next above the previous one. This recoating method (reapplying resin to the build surface) is called *dipping*, and it is very frequently used [7].

Two main problems appear in the use of this technique. First of all, it is really difficult to control the layer thickness, which depends on gravity, viscosity and surface tension of the resin. In order to avoid this problem, a sweeper blade as the one shown in picture Figure 9 is used, although it considerably decreases the process's speed. The second problem is the oxygen inhibition, i.e., the air diffuses into the outer layers of resin while printing, preventing the print from fully curing. This problem can be avoided by using a transparent glass window as the one explained in the vector scan method. By using the mentioned glass window, it is possible to avoid the presence of oxygen during the

polymerization process, so that better results can be obtained. Nevertheless, it might appear a new problem; adhesion of the polymer to the glass window.

3.2.2.2 Bottom up orientation approach

There are two main differences between this approach and the top down orientation. First of all, in this case the light is projected from below, see Figure 10. The second difference is the platform movement. While in the previous case the movement was downwards once the corresponding layer had been polymerized, in this method it is translated upwards. This sort of recoating method is called *by gravity* [7].

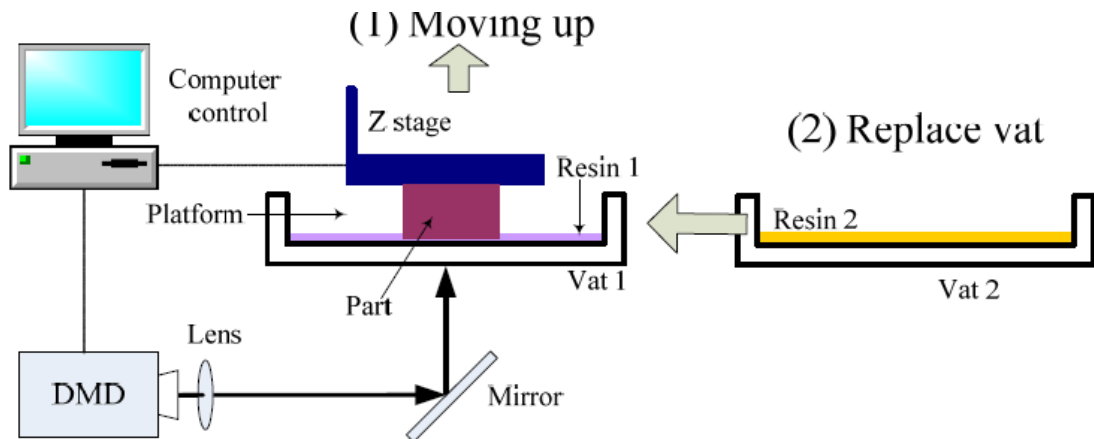


Figure 10. Schematic of bottom-up orientation approach, where the Z-stage moves upwards and the light is projected from below [18]

The main advantage of this method is that there is no more oxygen inhibition because the layer is polymerized between the bottom of the vat, and the previous layer, or between the resin vat and the platform, if the layer that is being polymerized is the first one. Nevertheless, the adhesion problem to the vat's bottom still exists, so coating materials that reduce the force between the polymerized layer and the bottom's vat will have to be used in order to not damage the desired object.

Finally, it is important to highlight that by using this method, the layer thickness is not dependant anymore on gravity or the resin's viscosity. Moreover, as a sweeper blade is no longer needed, the process's speed will be increased.

3.2.3 Two photon polymerization

By using this method, which was first demonstrated in 1997, the desired object is created directly in the resin, not on its surface, which has certain advantages, such as the possibility of avoiding support structures, which leads to an increase of the process speed. It is an optical nonlinear phenomenon that happens when two photons reach the transition energy between the excited and the ground state. Figure 11 shows the schematic of this process:

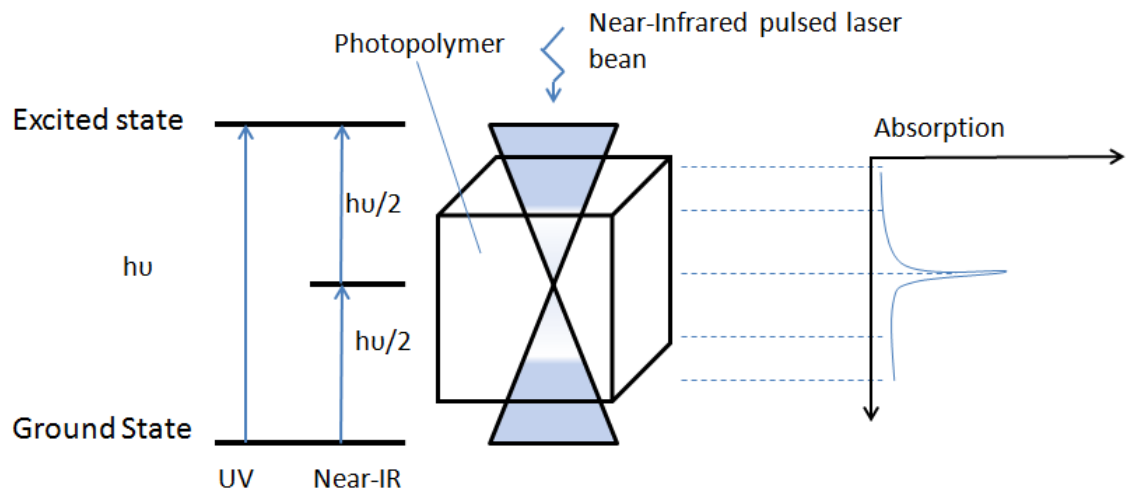


Figure 11. Two-photon process. Two photons reach the transition energy between the excited and the ground state

Only small samples could be created using this technique. Moreover, complex optical systems as much as adapted chemical media are needed to maximize the energetic density of the light beam under the surface.

3.3 Existing projection microstereolithography systems

3.3.1 Liquid crystal display (LCD) based projection microstereolithography

In 1996, the first LCD based projection microstereolithography machine was developed by Bertsch et al [7]. LCD is a flat panel that acts as a dynamic pattern generator. It consists of several chips which liquid crystal molecules orientation can be controlled in order to switch between transparent and opaque state. Table 1 presents some systems that were built using this technology:

Table 1. LCD based projection microstereolithography systems [7]

Research Group	Year	Special Features	Min. Feature Size	Min. Layer Size	Maximum Part Size	Vertical Build Rate
Bertsch	1997	LCD,Laser, 515nm	5 μm	5 μm	1.3 x 1.3 x 10 mm^3	110 layers in 90 minutes
Chatwin	1998	LCD,Laser, 351.1 nm	5 μm	Not reported	50 x50 x 50 mm^3	60 second exposure per layer
Monneret	1999	LCD,Lamp, 530nm	5 μm	10 μm	3.2 x 2.4 x 1.3 mm^3	60 layers per second

LCD presents several disadvantages, as their low transmission, only about 12.5% of UV light received from the light source, which is the reason why new techniques appeared in order try to increase the amount of UV light transmitted. Low resolution and the poor contrast of LCD also are disadvantages of this process.

3.3.2 Spatial light modulator (SLM) based projection microstereolithography

SLM is a special LCD component that has the possibility of using UV light source (this stereolithography technique operates in the UV (351.1 nm) [19]). A schematic of this process is shown in Figure 12:

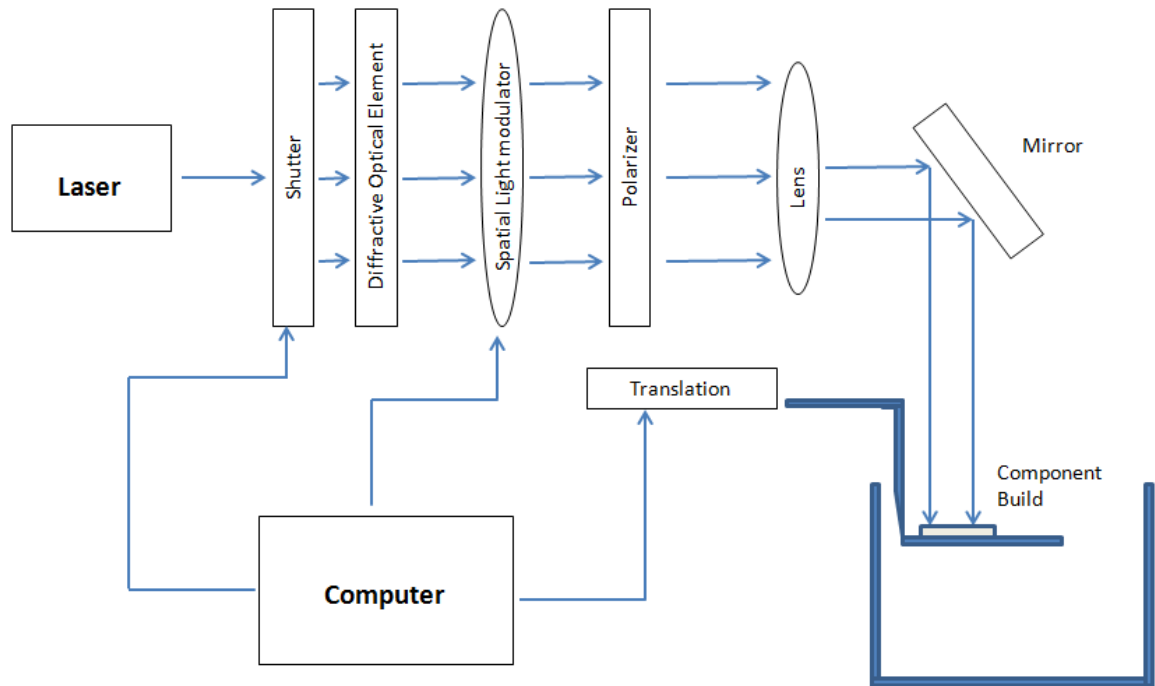


Figure 12. Schematic of SLM based projection microstereolithography. The final printed image will depend on the state of the SLM in every single moment [19]

In Figure 13, a microgear manufactured using this technique can be observed:

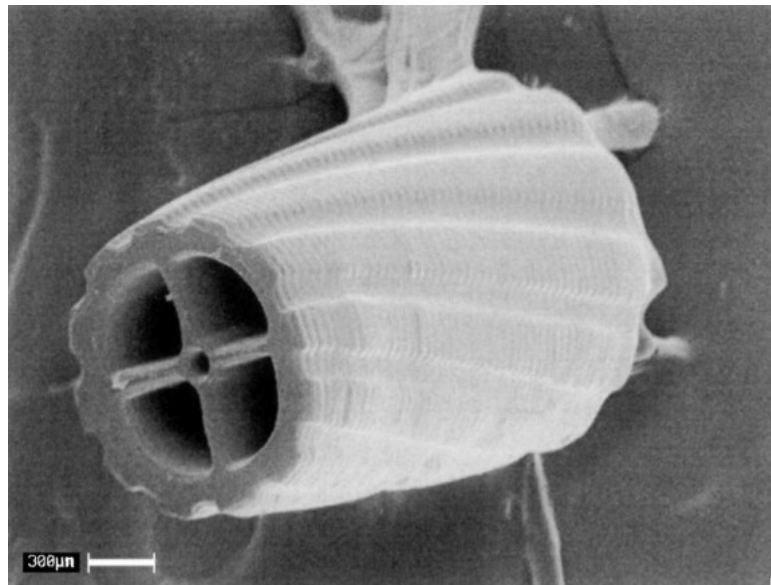


Figure 13. Scanning-electron microscopy photograph of the microgear printed using a SLM as a Dynamic Pattern Generator [19]

3.3.3 Digital mirror device (DMD) based projection microstereolithography

A DMD has several hundred of micromirrors on its surface, as shown in Figure 14, and each corresponds to a pixel of the image to be displayed. Each micromirror can rotate between $\pm 10-12^\circ$ to place it in an 'on' or 'off' position. In the 'on' position, the light coming from the source is reflected in the lens of the device causing the corresponding pixel to shine on the screen. In the 'off' position, the light is directed elsewhere (usually at a heat sink), making the pixel appear dark.

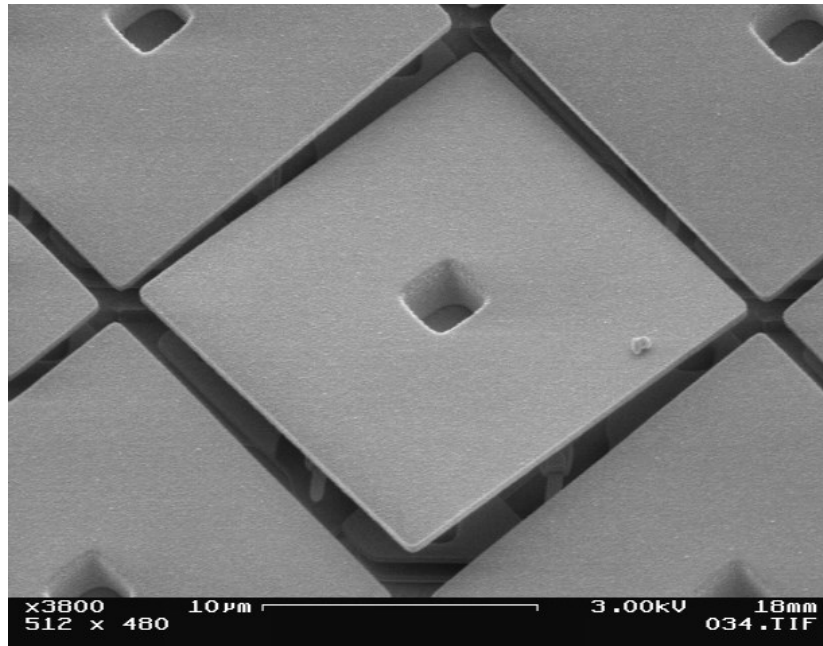


Figure 14. Micromirror from a DMD. The final image will depend on the state of all of the micromirrors that are part of the DMD

As an emerging dynamic mask, the performance of Digital Micromirror Device (DMD) is better than that of the LCD since DMD's fill factor of each pixel (85%) and its reflectivity (71%) are much better than those of the LCD (64% fill factor and 21% light transmission). In other words, when a pixel is in "active" or "on" state, the DMD can pass light more efficiently than the LCD [20].

DMD's surface is made of Aluminum, which reflects approximately 88% of the incident light [21], so they are much more efficient as dynamic pattern generators. Moreover, their speed between states is much higher compared with LCD's, which make them the superior choice. Some systems, based on this technique, that have already been manufactured are shown in Table 2:

Table 2. Based projection microstereolithography systems [7]

Research Group	Year	Special Features	Min. Feature Size	Min. Layer Size	Maximum Part Size	Vertical Build Rate
Chen	2012	DMD,Lamp, visible	400 μm	100 μm	48 x 36 mm^2	180 mm per hour
Kang	2012	DMD,Lamp, UV	Not reported	Not reported	14.6 x 10.9 mm^2	Not reported

3.3.4 Liquid Crystal on Silicone (LCoS) based projection microstereolithography

LCoS technology uses a liquid crystal display and a silicon device. The screen is applied on the device, so that it applies an electric current on the particles of liquid crystal and changes its polarization so that they stop or not pass the light of a lamp. The silicon device, in addition, has a reflective surface, in this way the light crosses the screen, impacts on that surface and is reflected. Applying different levels of voltage to the liquid crystal particles result in different levels of brightness between light and non-light, and the amount of reflected light forms the image. Thus, it can be said that LCoS technology combines the transmission technique, since the liquid crystal particles leave (or not) to pass the light, and the technique of reflection, since the reflective surface of the silicon device returns the light beam.

A schematic of the performance of this Liquid Crystal on Silicone device can be seen in Figure 15:

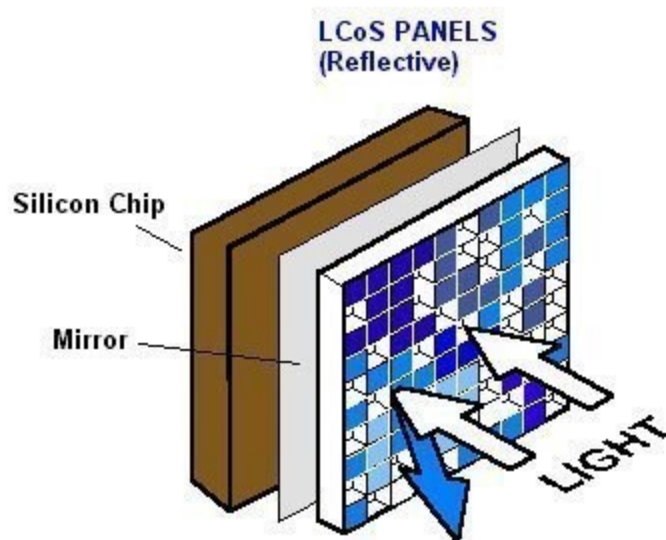


Figure 15. Schematic of the performance of this Liquid Crystal on Silicone devices [22]

4 Equipment and materials

4.1 Introduction

Figure 16 shows the schematic of the desired set-up:

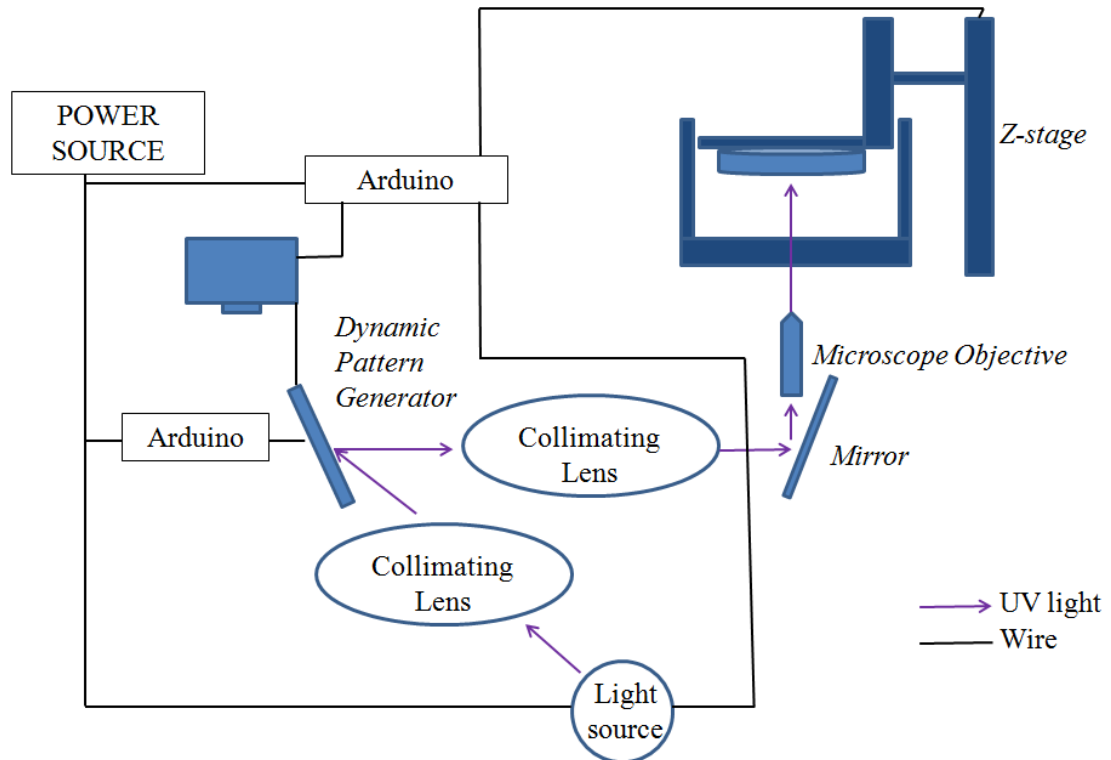


Figure 16. Set-up of a Mask Projection Microstereolithography 3D-printer

Main requirements for the design of the $MP\mu SL$ system include:

- The manufactured system must be able to cross-link photopolymer in a vat by the exposure of light at a certain wavelength
- As a certain speed is expected from the desired system, entire 2D contours are projected and the entire layer is cured simultaneously, i.e., mask projection method has to be used
- In order to get a high resolution, sub- $5\text{-}\mu m$ features are required
- The process should be automated with a simple system operation

In order to achieve all those goals, Table 3 shows a matrix where different alternatives are proposed for each one of the components necessary for the manufacture of the system:

Table 3. Different solutions for each one of the components of the M μ SL system [7]

	Solutions			
Light Source	Lamp	LED		Laser
Conditioning Optics	Homogenization	Collimation	Filtering	Beam Expansion
Pattern Light	LCD	DMD		LCoS
Projection Orientation	From Above		From Below	
Imaging Optics	Image Expansion		Image Reduction	
Recoat	By gravity	By spreading	By pumping	By dipping

Later on, we will proceed to explain each of the components selected for the system to be constructed. Apart of the components previously mentioned, a resin vat, a platform and an elevation device are also required for the system.

The projection orientation selected is from below, i.e., bottom-up orientation.

4.2 Light source

As shown in Table 3, three different light sources can be used: lamp, LED or laser. In order to select the best option, factors such as the emission spectrum, the intensity of the light and the divergence and intensity profile must be analyzed.

A LED was chosen as the light source in this system. Energy efficiency is clearly one of the biggest advantage of LEDs over the rest light sources. The energy consumption for polymerization of certain volume of material by LEDs is much lower than lasers and mercury lamps. Low heat dissipation, shorter starting time, longer lifespan, compact size and low cost are other advantages that lead to choose LED technology over other conventional light sources [23].

Moreover, another great advantage of using LEDs instead of using a projector lamp is the fact that the hotspot compensation can be avoided. It occurs when using a video projector lamp, of which intensity is not uniform, and an intensity corrected background image must be used [8].

Figure 17 shows the actual LED selected (410 nm):

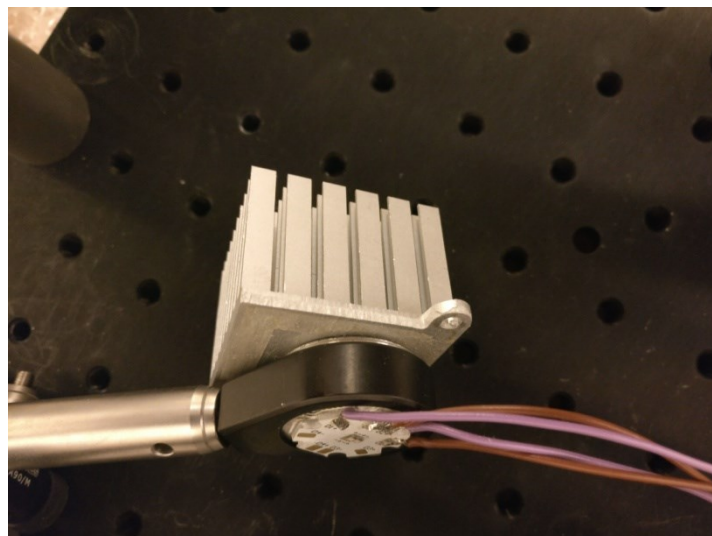


Figure 17. LED selected as light source (410 nm)

The functioning of the LED is controlled by an RCD-24, see Figure 18., which is a step-down constant current source designed for driving high power white LEDs. This device receives a signal from an Arduino to turn the LED on or off; when the output of Arduino connected to the RCD (number 2 in Figure 18.) is set as HIGH, the LED is off, nevertheless, when it is set as LOW, the LED is on. The LED will be connected to the RCD-24, the one will be connected to a 12V power source and to an Arduino (by a resistor of high resistance), as it is shown in Figure 18:

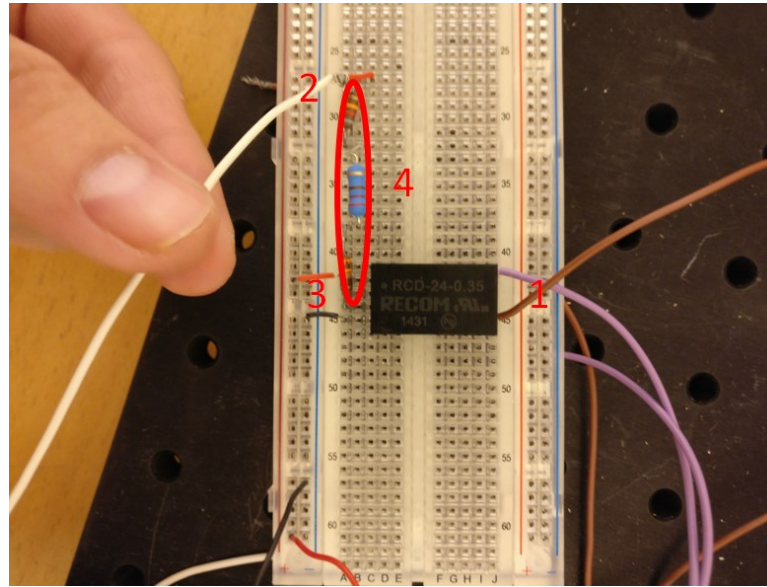


Figure 18. RCD connections. 1: LED wires, 2: Arduino wire, 3: power source and 4: resistors

The main purpose of the RCD is to provide a constant intensity to the LED (0.35 A), as much as control its functioning due to its connection to the Arduino by the PWM pin.

4.3 Digital micromirror device

Due to the reasons mentioned in the previous section, DMD technology has been chosen as a Dynamic Pattern Generator. In this particular case, the selected DMD can be found in a commercial projector, Optoma HD20 (HD (1080p), 1700 ANSI Lumens, Home Theater, the one features a native 1080p resolution (1920 x 1080 pixels)[29].)

The operation of this device is very simple. Light arrives at a 24° angle to its normal vector. Depending on its position ($+ - 12^\circ$), the light will bounce and will be directed to polymerize the photopolymer, or on the contrary, will be diverted, as it can be seen in Figure 19. The DMD system will be formed by thousands of these mirrors, one for each pixel of the desired 2D cross section.

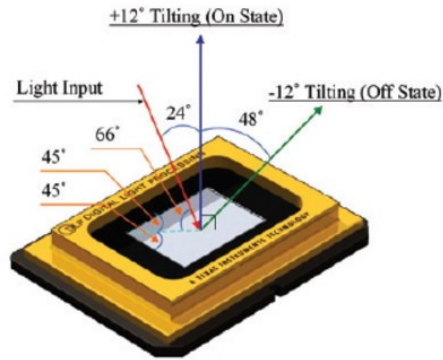


Figure 19. Schematic of DMD. Depending on its position, the light will bounce and will be directed to polymerize the photopolymer, or on the contrary, will be diverted [24]

Figure 20 shows the actual DMD used for this project, where the red line shows the path followed by the light that finally reaches the photopolymer.

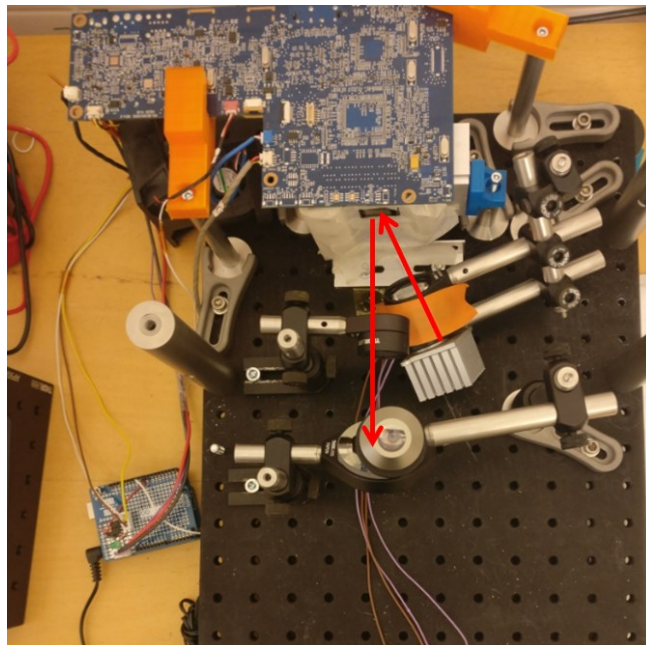


Figure 20. DMD used. The red arrows show the path followed by the light that will polymerize the photopolymer, this is, the light bounced by the micromirros in activate mode

4.4 Optical components

As shown in Figure 21, the light produced by a source of light is highly divergent, which decreases the resolution of the desired object:

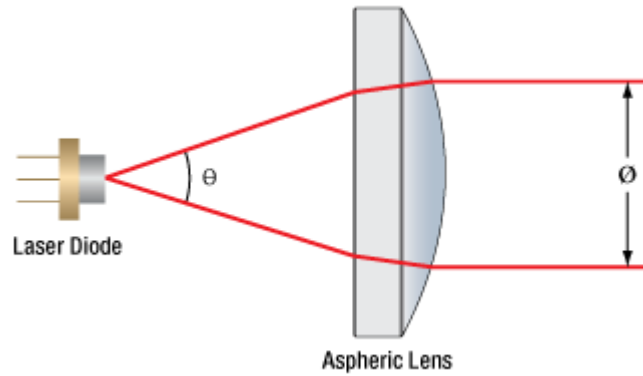


Figure 21. Divergent light. These lenses avoid light's divergence, i.e., keep it parallel [25]

In order to get rid of that divergence, it is necessary to use some lenses which collimate the light, i.e., make it parallel. The lenses that follow this requirements are aspheric lenses, Figure 21. The criteria followed to chose the most suitable ones has been based on the focal length, determined by the desired set up. In this particular case, the lens chosen to be located in between the LED and the DMD is the one shown in Figure 22:



Figure 22. AL3026-A - Ø30 mm aspheric lens. Manufacturer: Thorlabs [26]

Due to its short focal length (26mm), it is not possible to use the same lens after the DMD. This is why a 75mm focal length lens, as the one shown in Figure 23, was chosen:

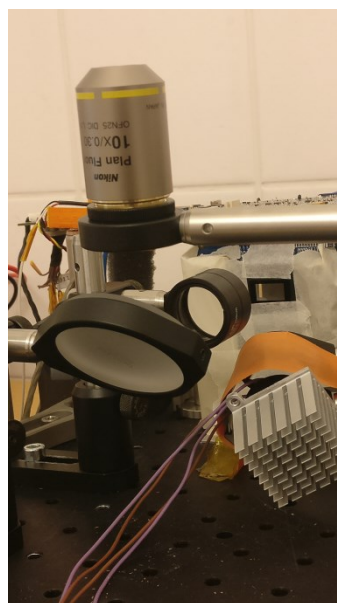


Figure 23. 75mm focal length lens

The second optical component used is the microscope objective. Once the light has been collimated, this microscope focuses it in the interface between the resin vat and the resin, to obtain an image as sharp and centered as possible. For this Master's Thesis, the microscope objective selected is the one shown in Figure 24, the one can work with UV light (as the light source used has a 410nm wavelength):



Figure 24. N10X-PF - 10X Nikon Plan Fluorite Imaging Objective. Manufacturer: thorlabs [27]

4.5 Resin vat

As the approach selected is the bottom-up orientation, the main characteristic of the resin vat is the transparency, so the light can pass through it and photopolymerize the photopolymer. It is also necessary that the bottom of the vat is as flat as possible so that it facilitates the polymerization layer by layer.

Finally, as mentioned before, with this kind of approach it is possible for the polymer to stick to the bottom of the vat, damaging the desired object. That is the reason why, either a special material is required in order to avoid it, or special coating materials must be used between the bottom of the vat and the polymerized layers.

4.6 Platform

The platform is the device where the first layer is polymerized. It also serves as support on which the desired object will be manufactured. The one used in this project is shown in Figure 25.



Figure 25. Platform used. Device to which the first layer is attached to

The size should be as small as possible, since the moment when the middle part of the platform touches the resin vat can be determined more reliably when the platform is lowered into the resin at the start of the fabrication process. The smaller the platform is, the less resin can be trapped beneath the platform. However the platform should be large enough to ensure sufficient attachment of the base layer to the platform. [8]

4.7 Elevator device

In the bottom-up approach, the first layer is polymerized over the platform. Once it has been polymerized, the platform elevates and the next layer is polymerized attached the previous one.

An elevator device is needed to scroll up the platform and create a new layer under the previous one. In this thesis, a stepper motor and a linear guide are used:

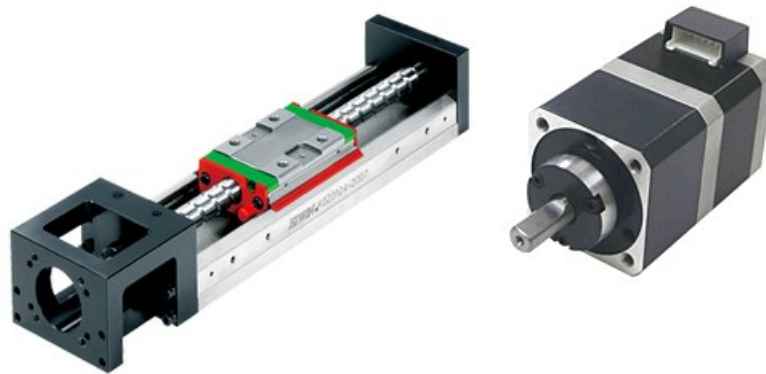


Figure 26. a) linear guide (Movotec: KK4001P-100A1) [28] and b) stepper motor (Movotec: PK244PDA-P10-L) [29]

The motor is a 200-step-stepper motor attached to a 10:1 gearbox, see Figure 26.b. This is, 2000 steps are required in order to obtain a whole revolution. As the linear guide, Figure 26.a, attached to the stepper motor has a 1mm lead:

$$\frac{1 \text{ mm}}{2000 \text{ steps}} = \frac{0.5 \mu\text{m}}{\text{step}} \quad (13)$$

So it has been proved that that the step size accuracy ($\frac{0.5 \mu\text{m}}{\text{step}}$) is in agreement with the $\frac{1 \mu\text{m}}{\text{step}}$ requirement for $P\mu SL$.

Figure 27 shows the coupler used to transmit the movement between the stepper motor and the linear guide. Moreover, another structure has been built (white part in Figure 27) in order to ensure the attachment between both parts. That structure has been built with *U-Print* (Stratasys), a commercial fused deposition modeling 3D printer that allows a great part quality.

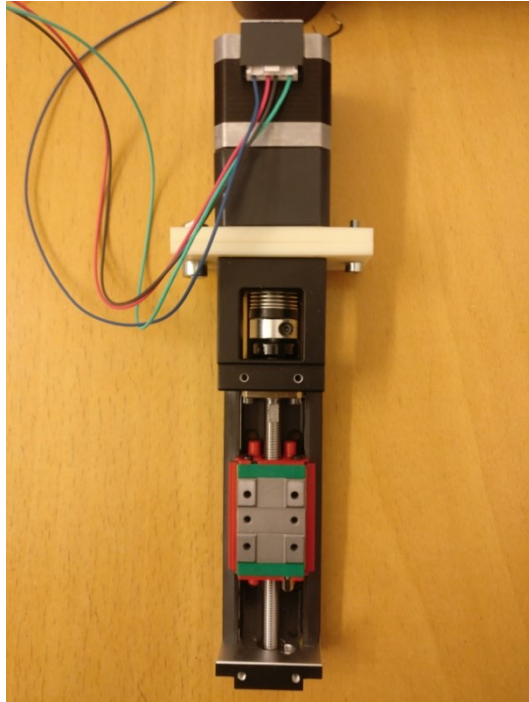


Figure 27. Coupling between stepper motor and linear guide. This device transmits the motor's movement to the linear guide

4.8 Electronic components and software

The electronic parts were provided by PhD researcher Tuukka Verho:

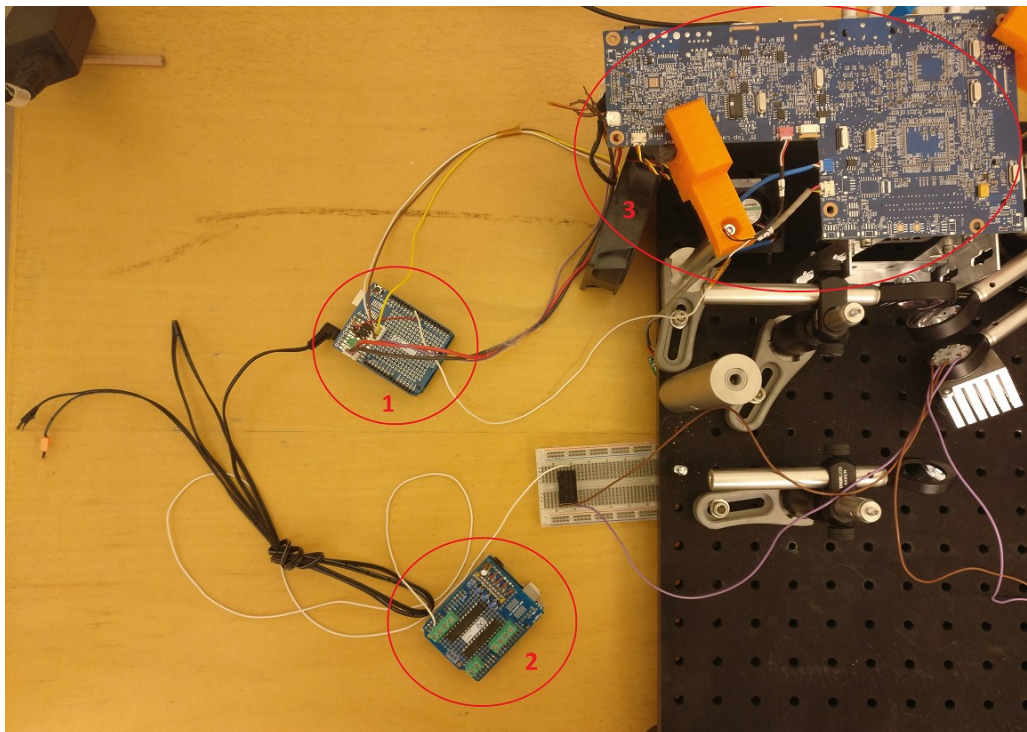


Figure 28. Electronic parts of the 3D printer. (1) Arduino 1, (2) Arduino 1, and (3) projector

As shown in Figure 28, the electronic part consists of 2 Arduino-1 and some parts of the projector which DMD is going to be used:

1. The function of first Arduino-1 is to trick the projector so it is possible to use its DMD but not its source of light (as the source of light that it is going to be used in this project is instead a LED). This Arduino must be connected to a 12V power source.
2. Second Arduino-1 is in charge of the step stepper motor and the LED, this is, it is responsible for turning on and off the led, as well as for the movement of the motor. As mentioned before, it is extraordinarily important a perfect synchronization between the LED and the motor, since if the LED emits light during the vertical movement of the platform, certain damages will appear on the desired sample. This Arduino also has to be connected to a 12V power source in order to work. Moreover, it must be connected to a computer, where the software will be running, to the stepper motor and to the RCD-24 that controls the LED. Once the machine was assembled, this part did not work as expected, so it was changed to an Arduino-Mega attached to a RAMPS 1.4 as shown in Figure 29:

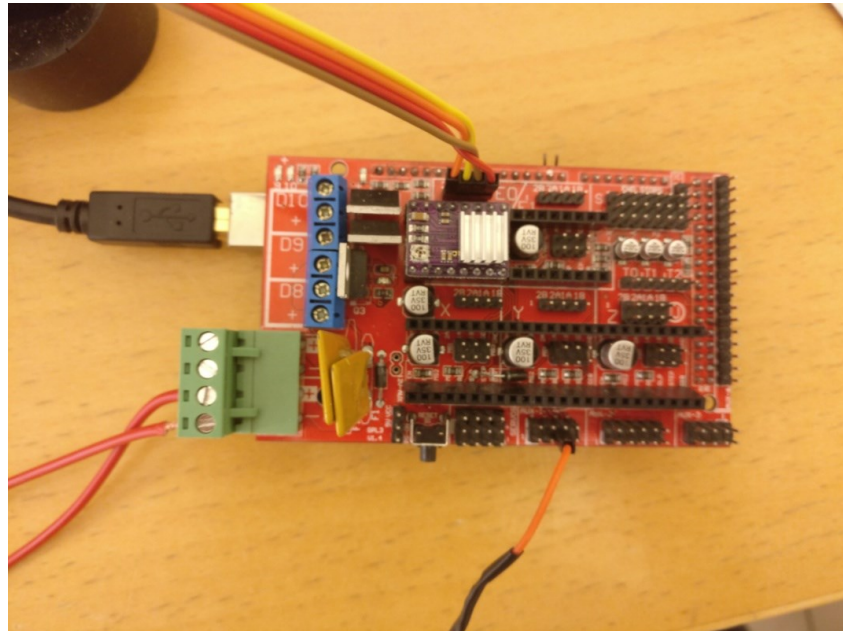


Figure 29. Arduino-Mega attached to RAMPS 1.4. This device will control the LED and the stepper motor to get a perfect synchronization between them

Once the Arduino was replaced, it was necessary to change the code previously provided, as in this new case the stepper motor will be controlled by a driver and not by the dual H-Bridge structure that had been built on the Arduino 1.

3. The electronic components of the projector are attached to the DMD in order to allow its functioning. The projector itself will be connected to the first Arduino-1, and to the computer via HDMI wire.

The software used in this Master's Thesis was written by doctoral candidates Pekka Lehtinen and Tuukka Verho. This software consists of Python and Arduino scripts (which has been modified), the ones are going to work together. The Python code cre-

ates a graphical user interface (GUI) that interacts with the Arduino code in order to control the stepper motor and the LED.

In order to make it work, the first step is to upload a folder that contains the cross section images of the desired object. There are several commercial software that will allow the user to obtain all the cross section images needed to print the sample. In this thesis, *Creation Workshop* [30] has been chosen.

Creation Workshop's interface can be seen in Figure 30.

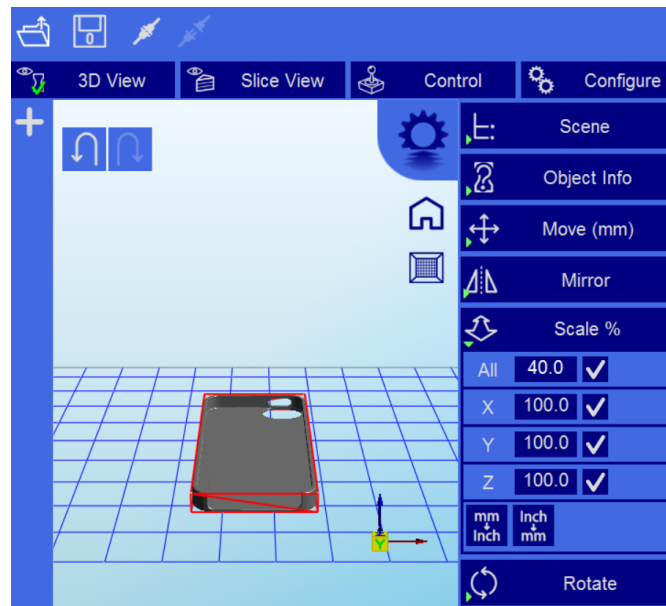


Figure 30. Creation Workshop's interface

In the software, several parameters can be settled, but we are only going to focus on the size and number of layers. The rest of parameters, as the speed, the exposure time or the motor movement will be controlled by the custom-made software.

The right orientation of the desired object is essential. This is, the bottom part should be on the surface determined but the xy axis, and it should increase in the positive direction of the z axis, otherwise, the sample will not be printed in a correct way. Once the desired object has been uploaded, and its size and position settled, the configure menu must be selected (top right). In that option, which interface is shown in Figure 31, a machine with the same resolution as the DMD that is going to be used must be selected (1920x1080 for this particular case).

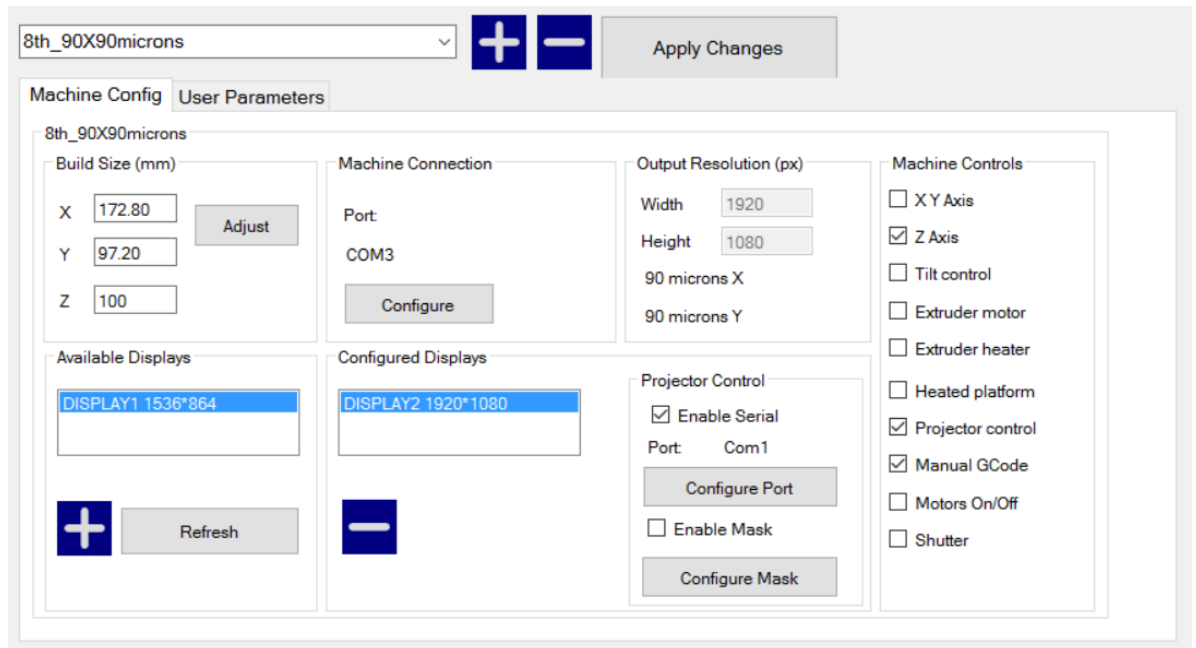


Figure 31. Configure menu


Once these steps have been followed, the last one is to click on the *Slice* button: . Afterwards, a folder with all the cross section images will be saved on the computer. Figure 32 shows 2 different cross section images of an specific object obtained by *Creation Workshop*:



Figure 32. Slices 100 (left) and 179 (right)

The next stage is to upload the cross-section images file on the Python software by clicking on the *Browse* button, which is shown in the top of Figure 33:

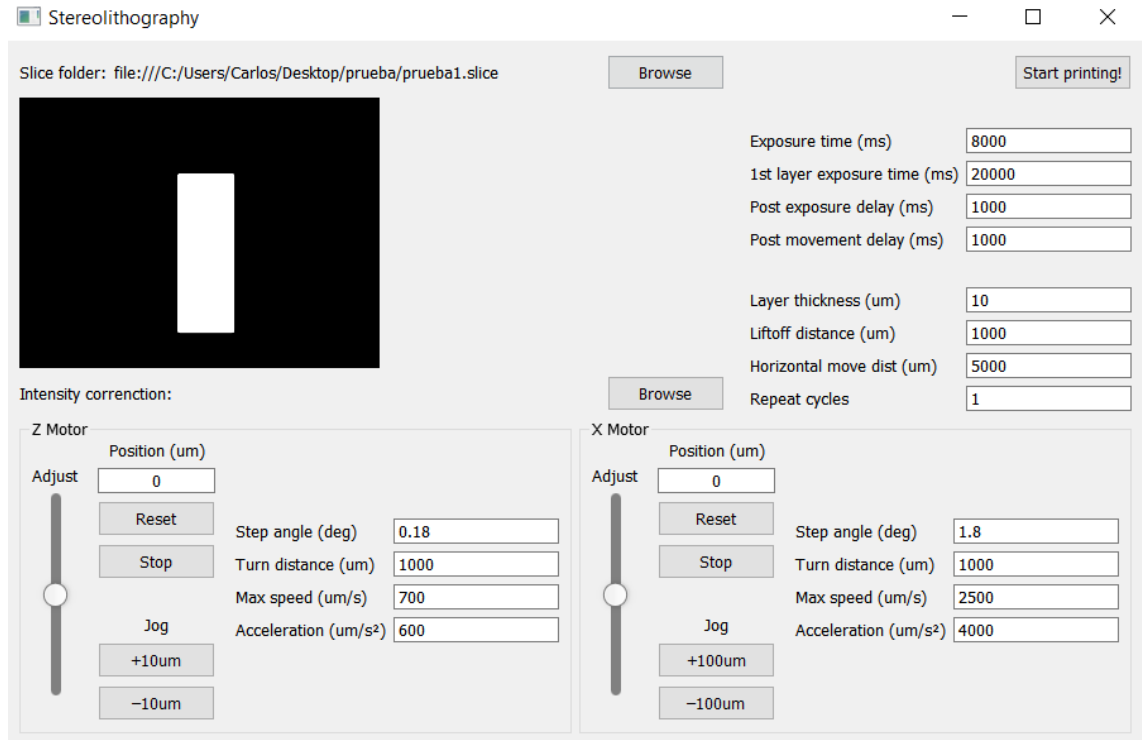


Figure 33. Python's software interface

Finally, after setting all the parameters, one can start the process by clicking on *start printing*. The computer's screen will turn black, and the 3D printer will start printing the desired object after pressing the 's' key. If for any reason it is desired to interrupt the process, it can be done by pressing the 'Esc' key.

4.9 Resins

HTM140V2 has been the resin used in this Master's Thesis. Its properties are shown in Table 4:

Table 4. HTMV2's mechanical properties

Property	Value
Tensile Strength	56 MPa
Elongation at Break	3.5%
Flexural Strength	3350 MPa
Heat Deflection Temperature	140°C

Moreover, as a bottom-up approach has been selected, a coating material will be needed in order to ensure the adhesion of the desired object to the platform, and not to the resin vat. It is important to remember that the desired object will get stuck to where the force is greater, so decreasing the force between the resin and the bottom's resin vat is necessary in order to ensure the proper functioning of the system. In this thesis, the selected coating material has been PDMS, which as shown in Figure 34, it is distributed on the surface of the resin vat forming a rather thick layer (about 5 mm):



Figure 34. Resin vat with a thick layer of PDMS

PDMS, whose properties can be seen in Table 5, is an ideal material due to its properties: it is optically clear, and, in general, inert, non-toxic, and non-flammable. Moreover, the ability of PDMS to inhibit free radical polymerization near its surface, due to the formation of a very thin oxygen-aided inhibition layer decreases the force between the desired object and the resin vat. [31]

Table 5. PDMS's properties

Property	Value
Mass density	$0.97 \frac{Kg}{m^3}$
Young's Modulus	360-870 Kpa
Tensile Strength	2.24 MPa
Specific Heat	1.46 KJ/Kg K

Due to this property of inhibition of the polymerization that oxygen presents, new techniques that allow to manufacture parts impossible to be manufactured through conventional processes have been developed (such as the one shown in Figure 35). Moreover, although those parts might be able to be manufactured by conventional 3D printing processes, these are very time consuming, and the mechanical properties of these parts might be affected by the orientation in which they were printed.



Figure 35. Part that can not be manufactured by conventional processes [32]

If an oxygen-permeable membrane is designed at the base of the resin vat, it is always possible to have a layer of fresh resin in the bottom, so that the time-consuming recoating process can be avoided. This technique called CLIP, whose schematic is shown in Figure 36, allows to print parts 25 to 100 times faster than conventional 3d printing processes.

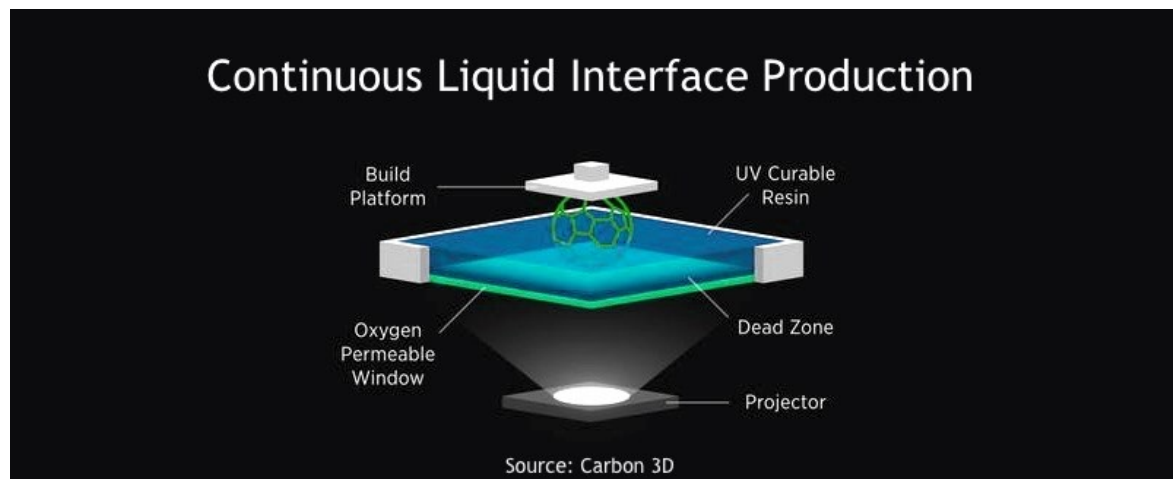


Figure 36. Schematic of the CLIP process. The permeable window creates a dead zone where the polymerization cannot occur [33]

4.10 Electronic Microscope

In contrast to conventional optical microscopes, there are the electronic microscopes, which resolving power is extremely high (250 times more than light microscope). The main difference between these two kinds of microscopes is the mechanism of image formation. While the image formation in the light microscope depends on the absorption of light (which is emitted from a light source), in the electron microscope it is based on the electron scattering (the ones are produced by a cathode which is placed at the top of the microscope) [34]. Due to the size of the samples that are going to be printed, it is going to be necessary to use an electronic microscope to be able to analyze them and study the obtained resolution.

We must thank the invention of the electron microscope to Max Knoll and Ernst Ruska, who in 1931 developed the first of them. As of that moment a great evolution of this

type of microscopes was lived, obtaining resolutions of the order of the 10 nm at the end of 1930's, and of the order of 2 nm in 1944 [35].

Within this technique, two different approaches exist; Scanning Electron Microscope (SEM), and Transmission Electron Microscope (TEM). In Figure 37, a schematic of the Transmission Electron Microscope is shown.

The electron gun, which consists of a cathode (which is normally a Tungsten filament) and an anode, acts as the electron source, this is, it generates the electron beam. Then, the generated beam is focused, and its size is modified by the condenser lenses (which are electromagnetic lenses) and the aperture.

The sample, placed above the condenser aperture, is traversed by the electron beam, allowing the passage of electrons in function of its structure. Then, the beam passes through the objective lens, which refocuses the beam after it passes through the specimen, and the projector lens, which amplify the image and focus it on the region of interest. Finally, the beam gets to the fluorescent screen printing the desired image on it.

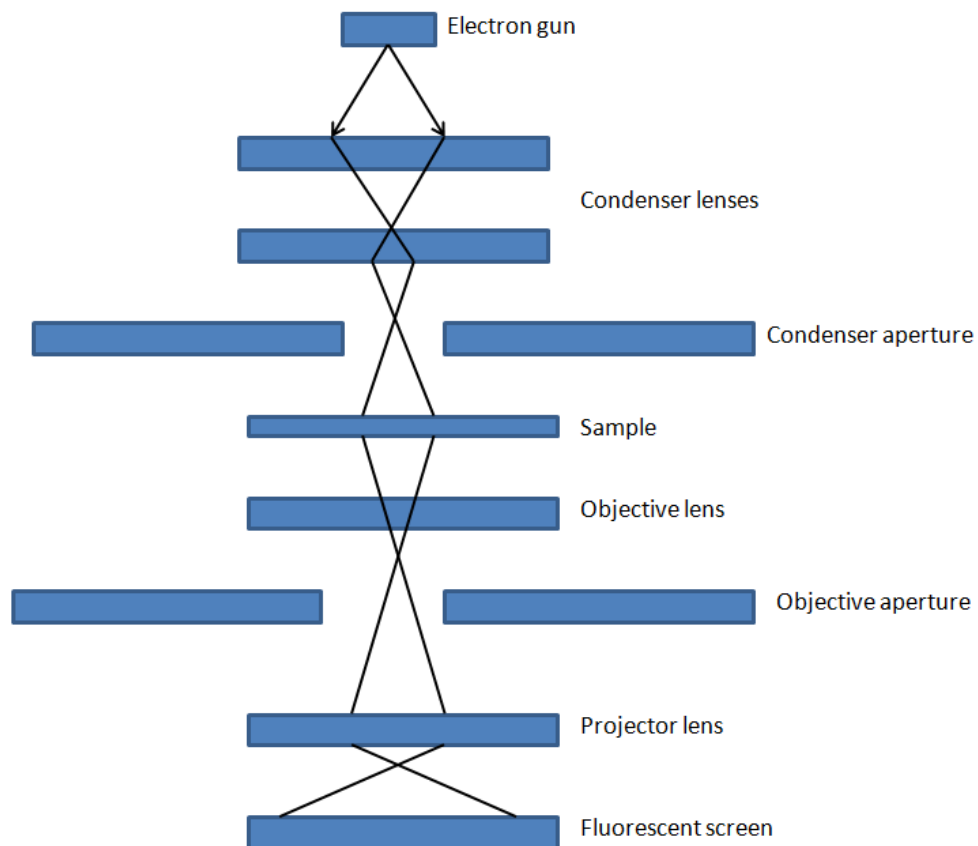


Figure 37. TEM's schematic. The electrons pass through the sample generating a pattern in the fluorescent screen [36]

On the contrary, the Scanning Electron Microscope, whose schematic is shown in Figure 38, presents a different approach:

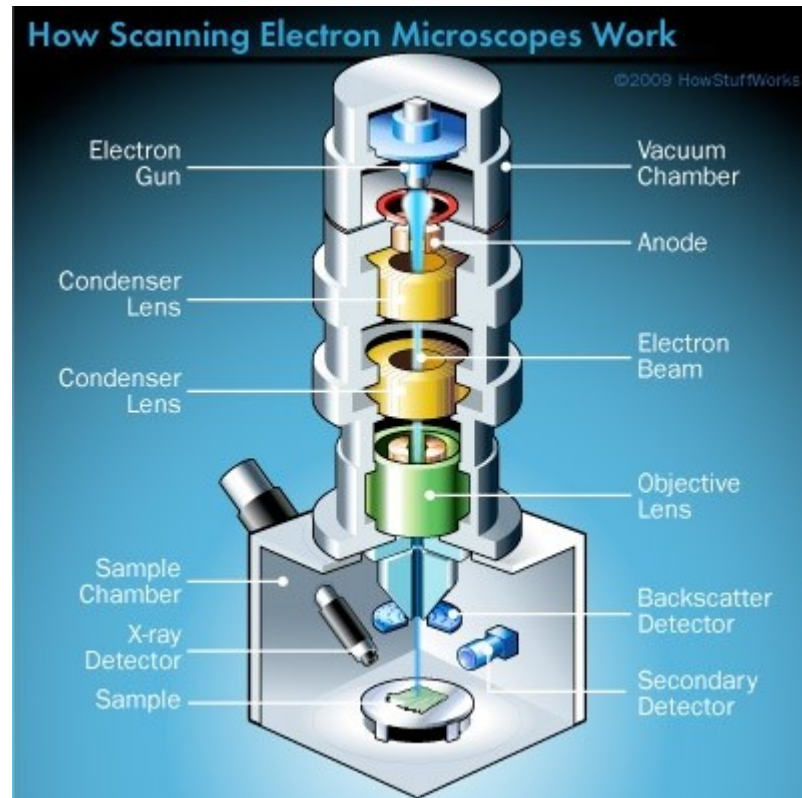


Figure 38. SEM's schematic. The electron beam scans the sample's surface [37]

As in the transmission approach, an electron gun, condenser and objective lens can be found as SEM's components. But in this particular case, the sample is placed at the bottom of the microscope, in the sample chamber. The sample chambers of an SEM does more than keep a specimen still. They also manipulate the specimen, placing it at different angles and moving it so that researchers don't have to constantly remount the object to take different images.

Finally, the characteristic components are the detectors, the ones register secondary electrons and produce a detailed image of the item's surface. This is, unlike of TEM, the electrons do not pass through the sample, but collide with it. Hence, they are only able to analyze the sample's surface.

In Table 6, some of most the significant differences between these two approaches are described:

Table 6. Differences between Scanning Electron and Transmission Electron Microscopes

SEM	TEM
It is used to analyze surfaces	It is used to analyze component's inside
Electron beam scans the surface	Electron beam passes through the sample
Produces 3D images	Produces 2D images
2nm average resolution	10 nm average resolution
Need to work in vacuum	Need to work in vacuum

5 Final set up

Figure 39 shows the final result of the 3D printer built. While some of the components have been bought, such as the microscope objective or the mirror, some others have been produced by commercial 3D printers, such as the connection between the motor and the linear guide, or the supports of the components of the projector.

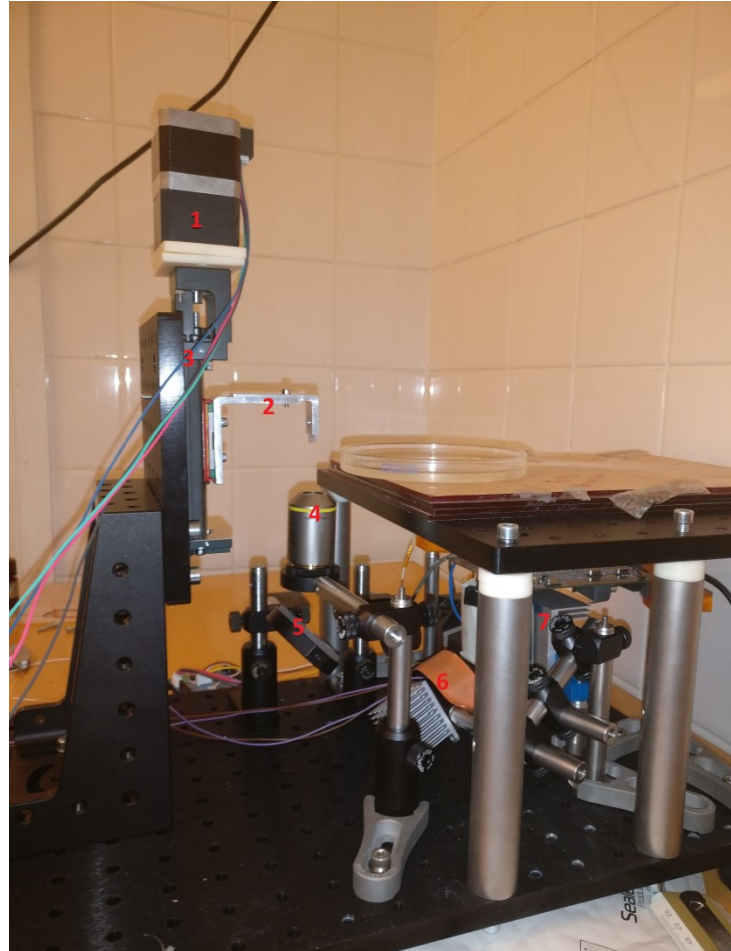


Figure 39. (1) stepper motor, (2) platform, (3) linear guide, (4) microscope objective, (5) mirror, (6) led with aspheric lens, and (7) DMD

As mentioned before, the light beam is produced by a LED and collimated by an aspheric lens. Then, it is reflected by the DMD depending on the position of its micro-mirrors. The rays that are bounced perpendicular to the DMD are collimated by a lens, and finally focused by the microscope on the resin vat once its direction has been diverted by the mirror, as it can be seen in Figure 40. Notice that the area surrounding the DMD has been covered with some paper in order to avoid the reflection of the beam of light produced by the structure, which could damage the final result:

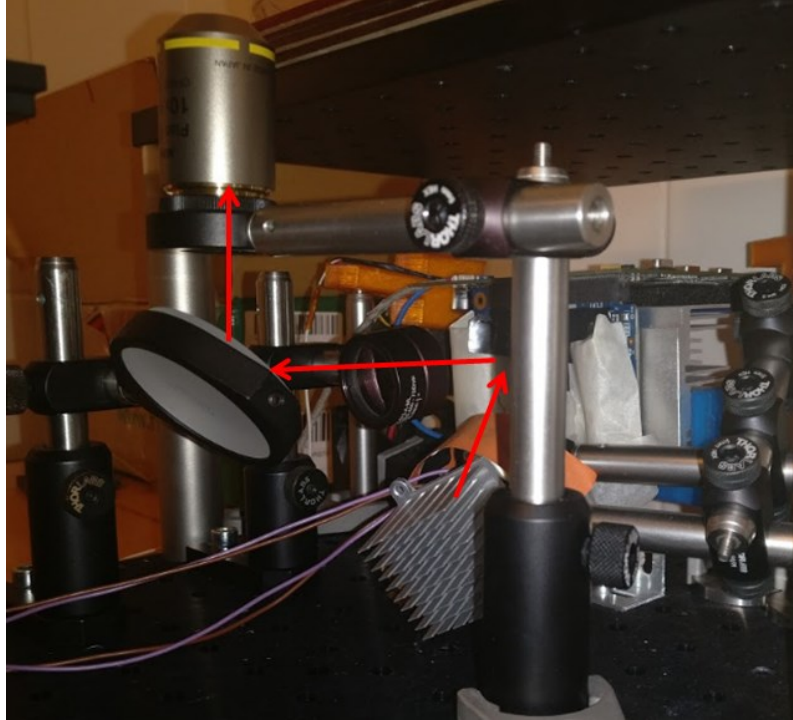


Figure 40. Path followed by the beam of light

Figure 41 shows the image that is to be projected on the interface between the resin and the resin vat, and the image that is actually produced. Due to the results obtained, it can be inferred that the focal length of the lenses has been calculated correctly, as much as the working distance of the microscope, this is, the distance at which it focuses the desired image:

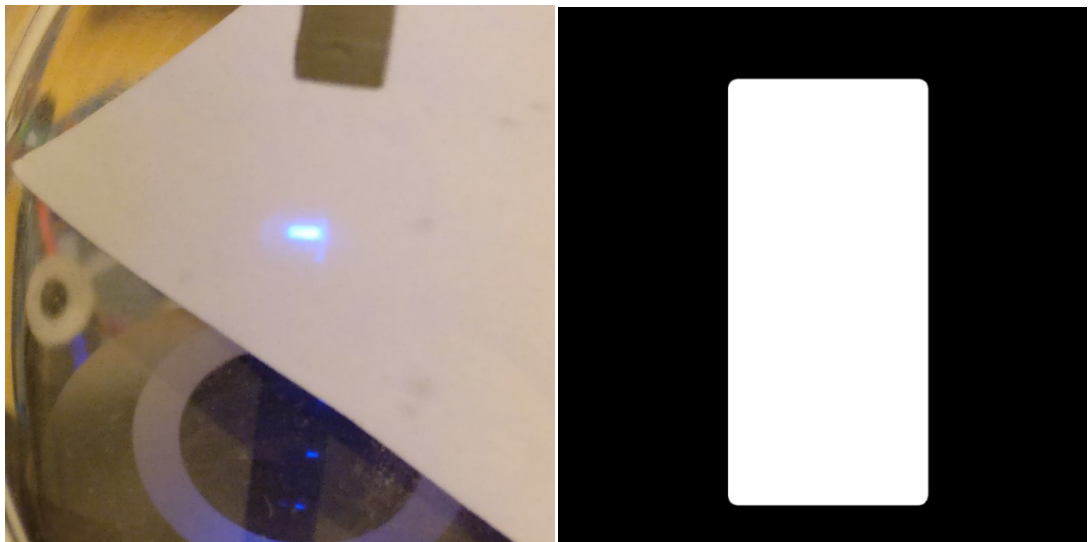


Figure 41. Projected and desired projected image

6 Experiments and results

Once the 3D-printer was built, the first step was to measure its horizontal resolution, this is, the area projected on the resin by one of the micromirrors of the DMD. In order to obtain this value, an image with the exact same resolution as the projector that has been used (1920X1080) was created. Different squares (24x24 pixels size) were drawn, separated by 8 pixels size lines, as it can be observed in Figure 42:

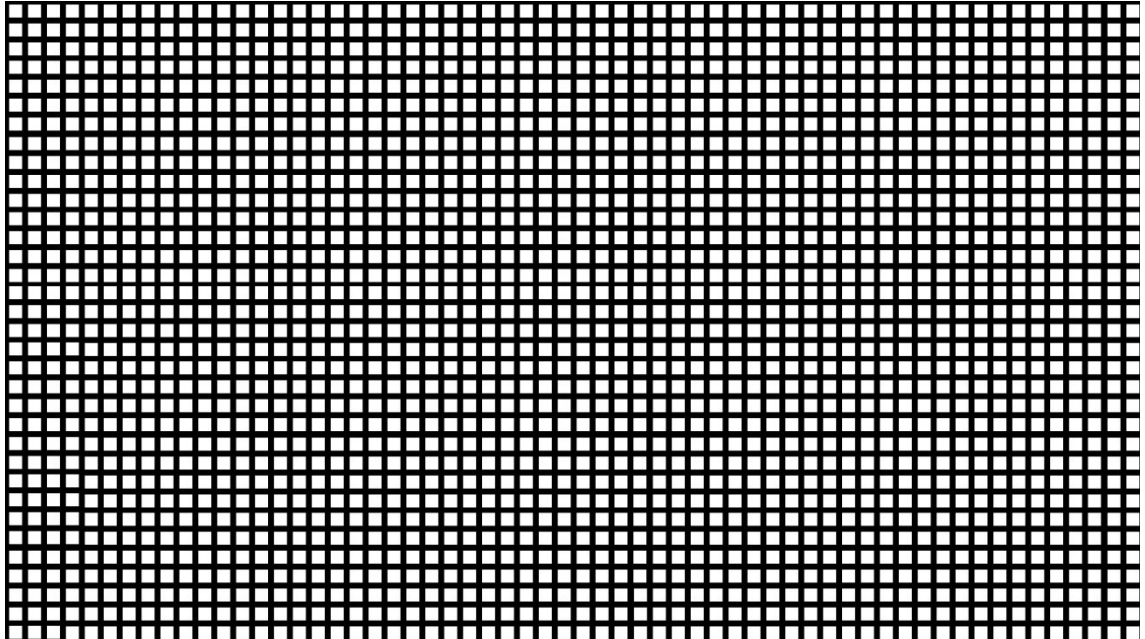


Figure 42. Draw used to determine the vertical resolution

This image was projected on the resin in order to obtain the same patron on it. So to determine the size of the squares previously mentioned, an optical microscope as the one shown in Figure 43 was used:



Figure 43. Olympus microscope BH-2

Figure 44 shows the image obtained with the microscope previously mentioned. It can be inferred that 128 pixels is equal to 269 μm , so the width of each pixel is around 2,1 μm , this is, each pixel represents an area of 4,41 μm^2 in the desired object:

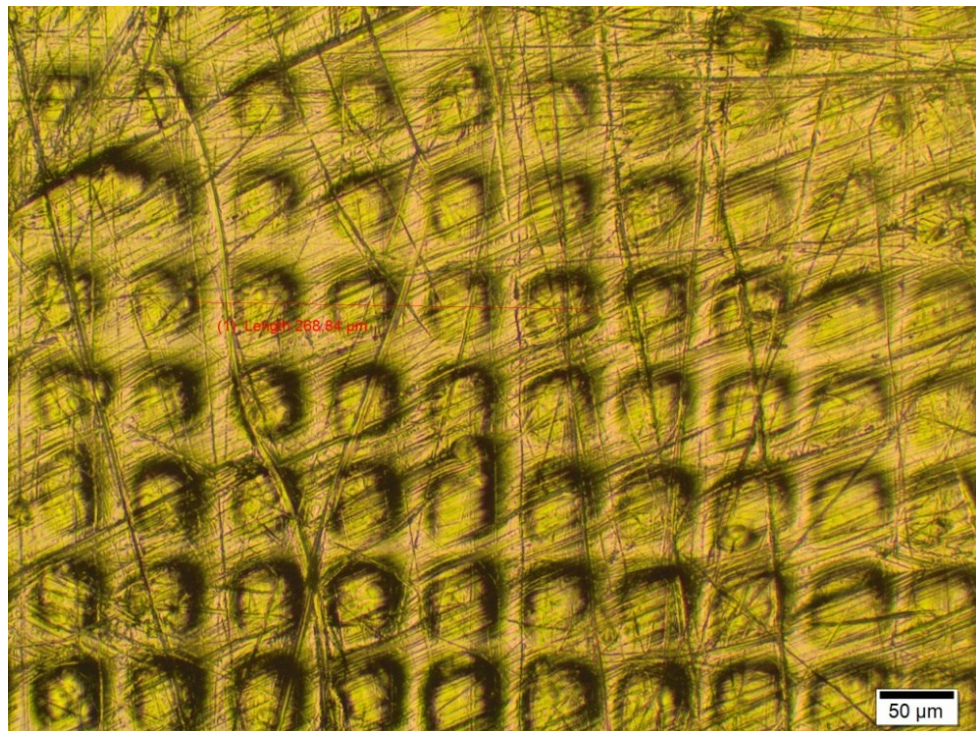


Figure 44. Patron obtained to calculate horizontal resolution

To be able to determine the real horizontal resolution, it is important not only to make sure the final set-up is focused, but also it is necessary to accurately determine the curing time of the resin to be used. That is the reason why certain tests were carried out:

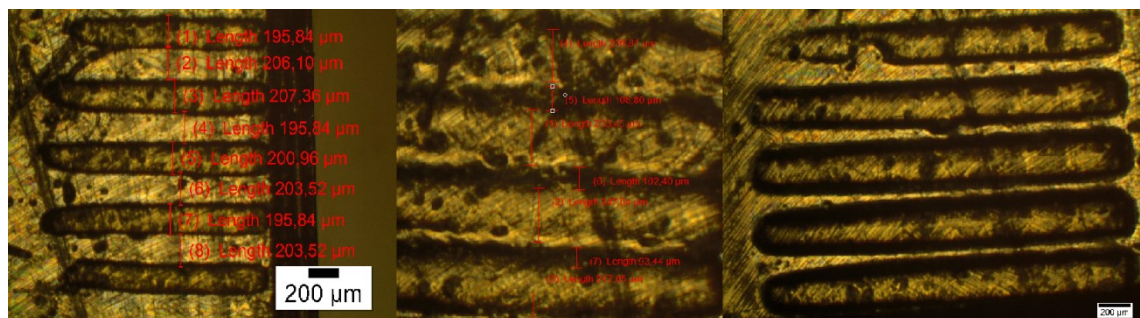


Figure 45. Problems on the horizontal resolution (from the left to the right: a, b and c)

Figure 45.a shows a pattern of parallel lines that has been printed in which the thickness of each of them is equal to the distance to the next. Figure 45.b shows what happens when the system is not focused, which results in certain areas not appearing, or if they do, it is blurry. Finally, in Figure 45.c it is possible to observe a case in which required the curing time has been exceeded, that is why the edges of the lines are thicker, and in some cases, there is hardly any space between one line and the next.

With the horizontal resolution achieved ($4,41 \mu\text{m}^2$), a $300 \mu\text{m}$ square can be easily printed, see Figure 46. It can be observed that the corners of the square shown are slightly rounded. The reason may be due to the lack of focusing or accuracy of the curing time calculated. This means that even after the tests previously mentioned, there is still room for improvement.

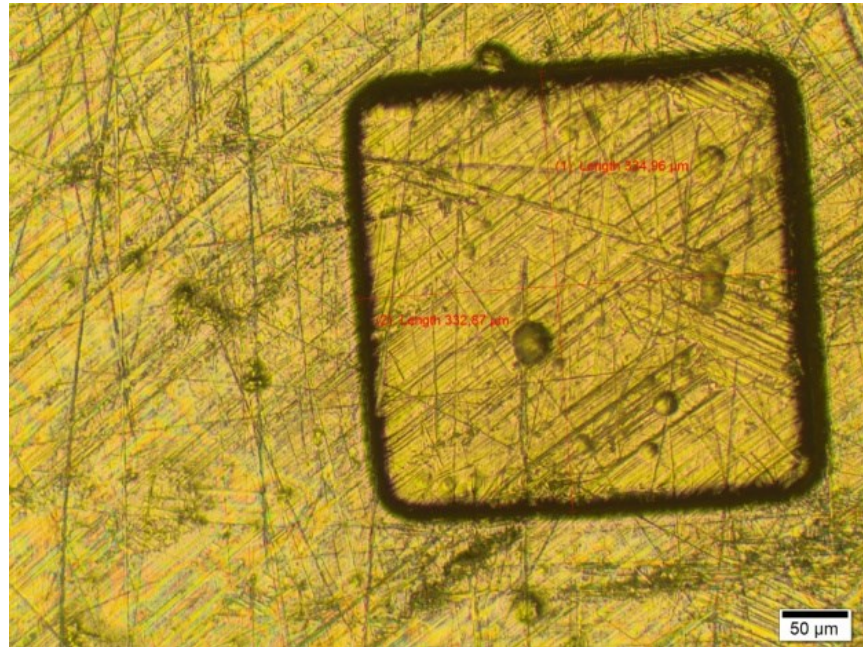


Figure 46. Printed square

It is important to emphasize the reason why an optical microscope, instead of an electronic one, has been used to analyze the surface of the printed samples. The main reason is its conservation. When studying the surface with a SEM microscope, the samples melt because of the large amount of energy that penetrates on them due to the laser, as it can be seen in Figure 47.

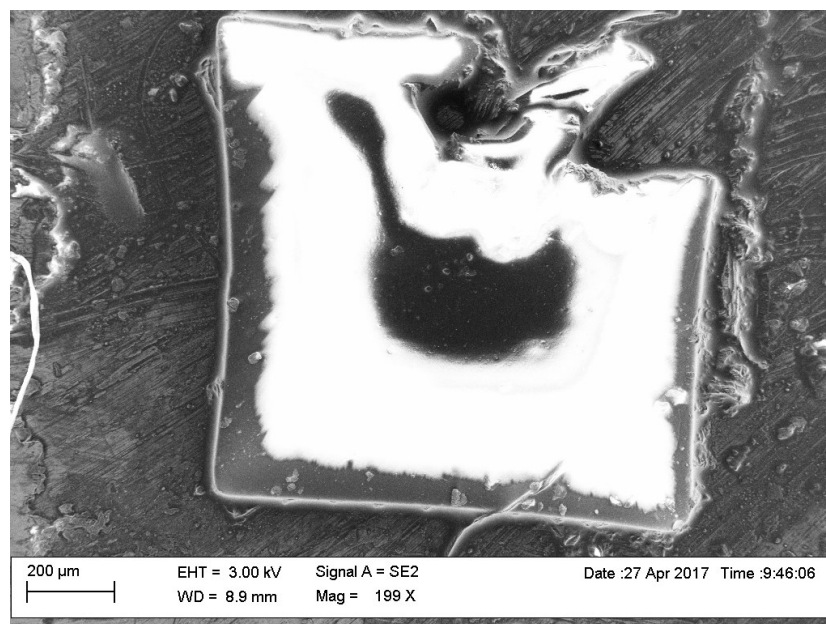


Figure 47. Damaged sample due to the SEM microscope

On the other hand, if the aim is to analyze the thickness, the SEM microscope gives very good results, since the amount of energy absorbed by the piece is much lower. That is why this was the microscope selected to characterize the vertical resolution of the printer. Figure 48 shows the image obtained by using a SEM microscope to measure the thickness of a certain sample:

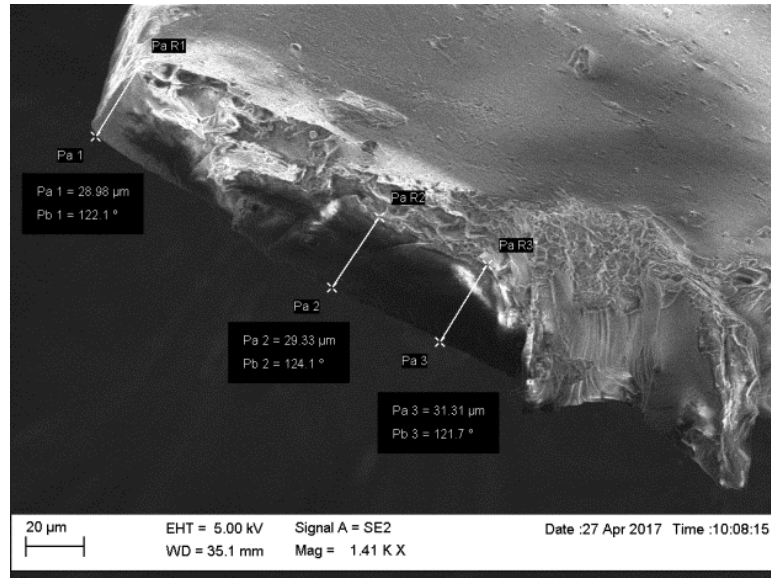


Figure 48. Thickness of a sample

To optimize the assembled machine, some samples were printed and analyzed to measure their thickness and cross-section area. Due to the high accuracy of the elevator device, there is a wide range of possibilities within the thickness of the desired samples. For example, they could be as thin as the one shown in Figure 49 (10 μm), or as thick as the one shown in Figure 50 (100 μm):

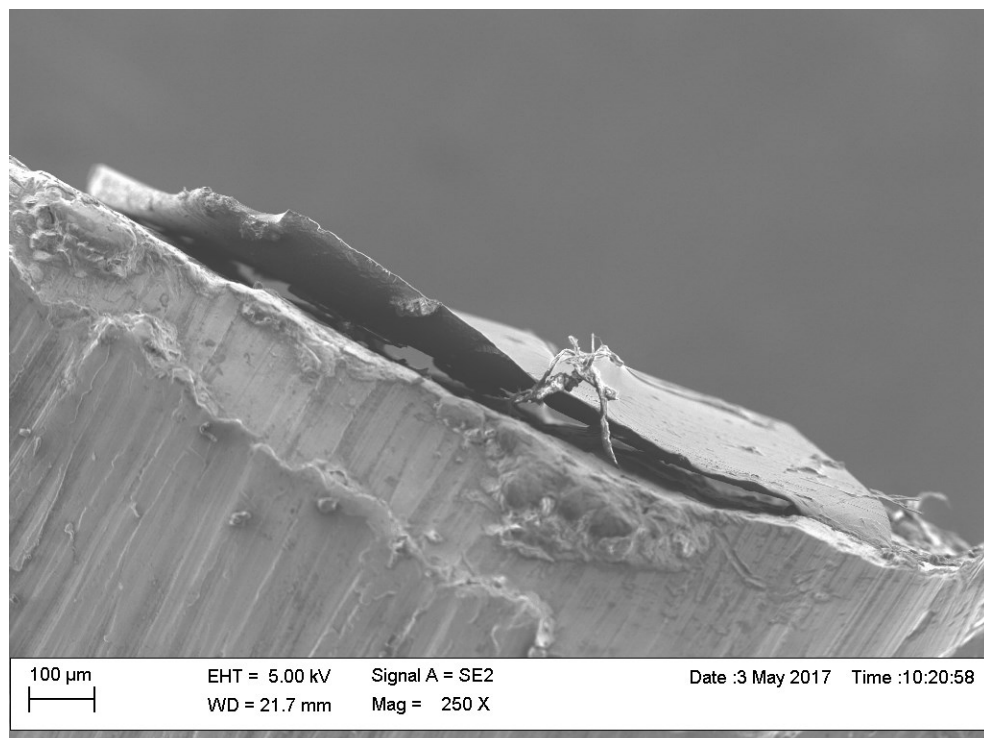


Figure 49. 10 μm sample thickness

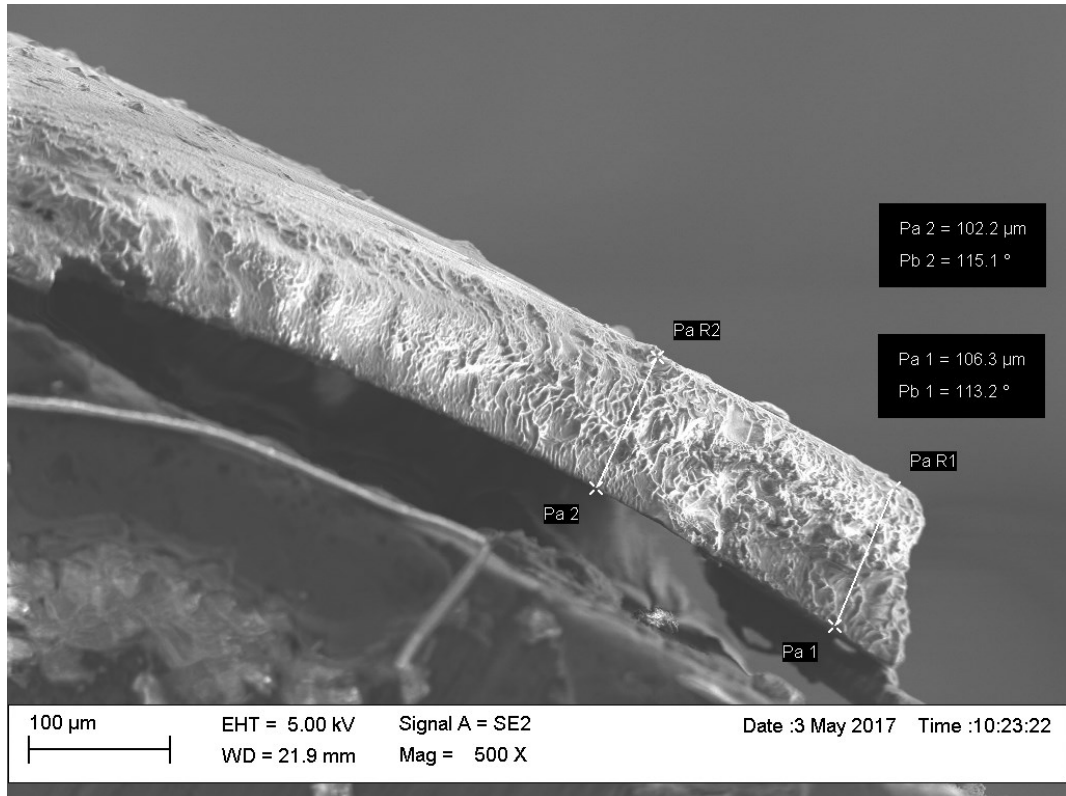


Figure 50. 100µm sample thickness

The printing of samples of high thickness using only one layer is directly related to the resin to be used. In this case, a resin that allows a great penetration of ultraviolet light from the LED has been used, but if one wishes to use another with a much lower penetration capacity, it would not be possible to obtain that sample with a single layer. Instead, several layers should be printed attached together until the desired thickness is reached.

Different size layers can also be obtained, for example, combining squares with a different cross section area, as shown in Figure 51:

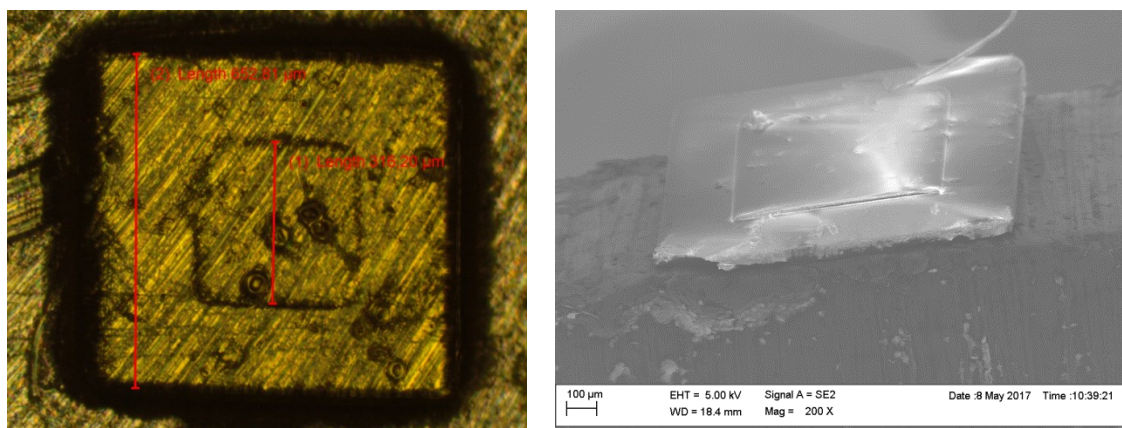


Figure 51. Combination of different cross section areas

The thickness of the sample was analyzed with an electronic microscope and the results are shown in Figure 52:

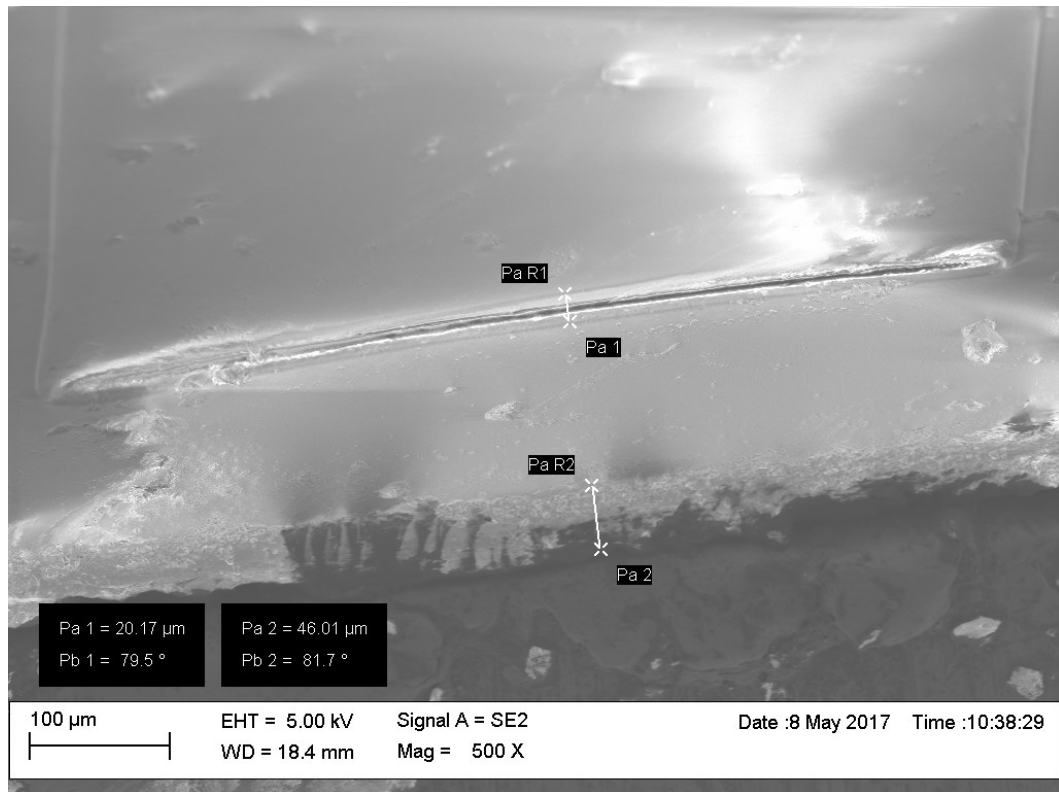


Figure 52. Analysis of the thickness. Three layers of 20 μm each

Three different layers have been printed in the image above; each of them of 20 μm . Two of them form the base adhesion plate, while the third one, which is smaller, is attached to them.

It is also possible to build more layers with different sizes, as shown in Figure 53:

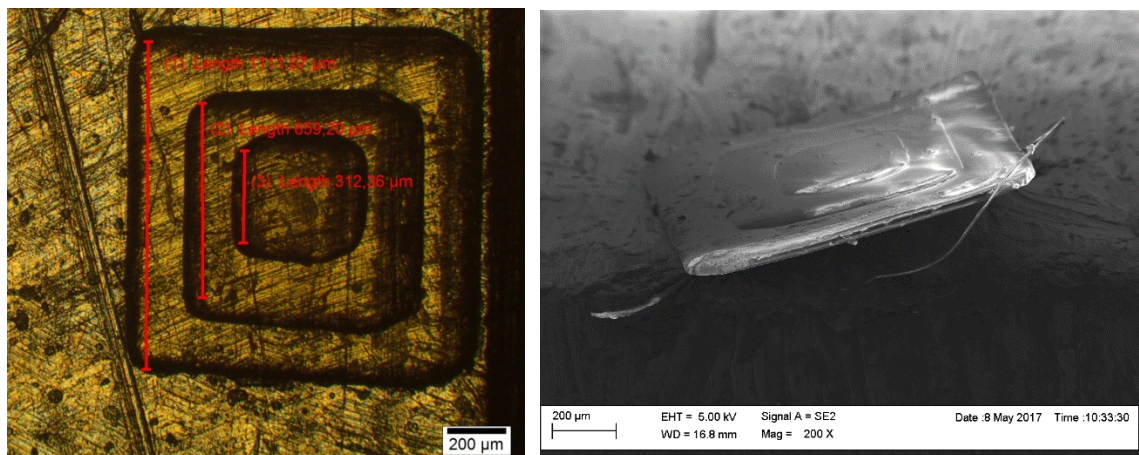


Figure 53. 4-layer sample

Once again, two 20 μm layers were printed acting as a base adhesion plate, while other two 20 μm layers with different dimensions were printed attached to them. Figure 54 shows the thickness of each layer:



Figure 54. Analysis of the thickness. Four layers of 20 μm each

Finally, different shapes can also be combined in order to obtain samples with a more complex geometry, as shown in Figure 55:

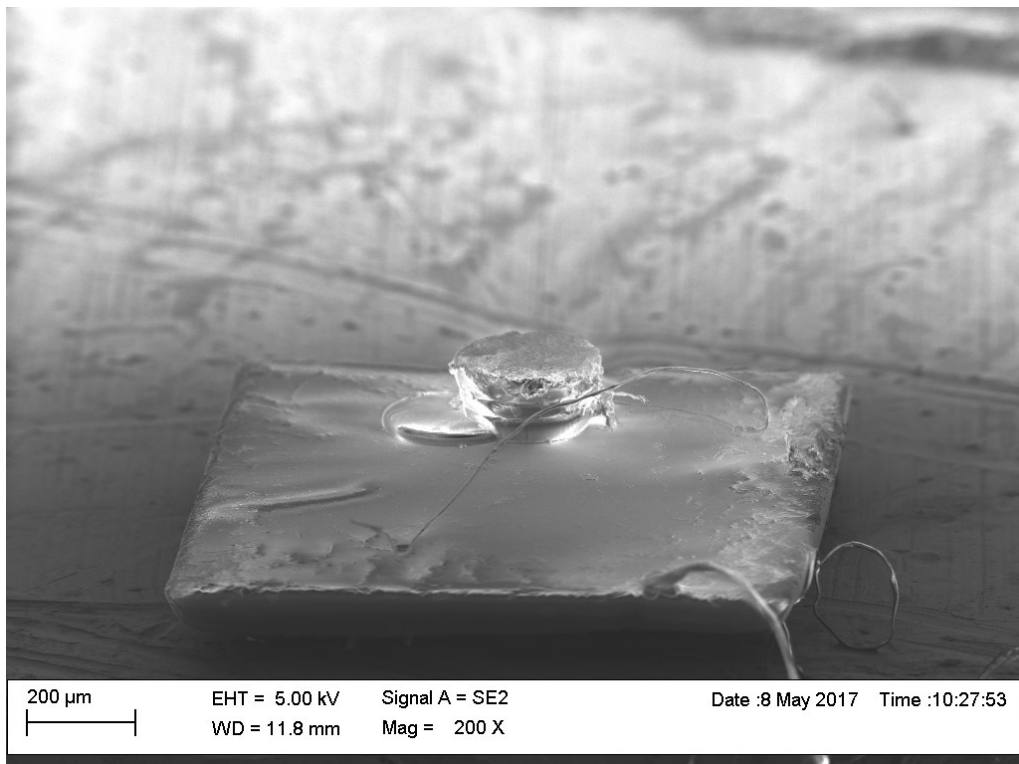


Figure 55. Different geometries

In this particular case, five layers of 20 μm were printed attached to another five rectangular layers of 20 μm each.

7 Summary and conclusions

A low-cost mask projection microstereolithography 3D printer has been built (attached as Appendix 1 is the budget expended during this thesis without considering the VAT). A bottom-up orientation was chosen due to the advantages it offers, eliminating the influence of gravity and the surface tension of the resin on the final result, and being able to avoid the use of a blade to obtain layers of a certain thickness. However, this approach leads to the use of a coating material between the resin vat and the platform to promote the adherence of the desired sample to the platform. PDMS is an ideal material due to its properties: it is optically clear, and, in general, inert, non-toxic, and non-flammable. Moreover, the ability of PDMS to inhibit free radical polymerization near its surface, due to the formation of a very thin oxygen-aided inhibition layer decreases the force between the desired object and the resin vat.

The built prototype consists of a UV led with a wavelength of 410 nm. The light it emits is collimated by an aspheric lens, after which a DMD is established, which acts as a dynamic pattern generator. Afterwards, the rays of light projected by the DMD are collimated and focused in the resin to polymerize with a microscope objective. The final sample can be obtained by the combination of different layers, using a stepper motor and a linear actuator that allow the vertical displacement of the piece to be built. The motor used is a two phase stepper motor of 200 steps attached to a 10:1 gearbox, this is, 2000 steps are required to obtain a full turn of the motor. As the linear guide attached to the stepper motor has a 1mm lead, each step represents a 0.5 μm displacement of the elevator device, which leads to a high accuracy of the final set-up.

As for the electronic part, the printer is controlled by two Arduinos and a program written in Python. The function of one of the Arduinos is to trick the projector so that its DMD can be used, without its source of light. Additionally, a second Arduino controls the LED and the stepper motor. The program of this later Arduino was slightly modified since in this case the stepper motor is controlled by a driver attached to a RAMPS 1.4, instead of dual H-Bridge structure for which the code was written.

As for the assembly of the printer, it was started by the optical components; calculating the focal lengths of the lenses to be used, as well as the working distance of the objective microscope. Afterwards, the previously mentioned code was modified, and the electronic part began to be tested, until the wanted operation between LED and the motor was obtained. It is important to perfectly synchronize the LED and the motor, since if the LED emits light during the vertical movement of the platform, certain damages will appear on the desired sample.

When printing, it is necessary to enter in the program interface programmed with Python the cross sections of the piece to be constructed. For this purpose, in this thesis "*Creation workshop*" was the software chosen to slice the desired sample. Once the images have been entered in the Python interface, parameters such as layer thickness, stepper motor speed or curing time must be adjusted.

At the time of analyzing the printed samples, both an optical and an electron microscope have been used. The optical microscope has been used to analyze the cross section of the samples, since the SEM laser melt them so it was impossible to study them. However, to analyze their thickness, SEM is very useful, since in this case the section is much

smaller so the amount of energy absorbed is not significant and the samples are not damaged.

Once built, we proceeded to study how well the system was focused in order to try to obtain parts with the highest quality possible. Tests were performed to try to optimize the machine and determine the curing time needed for the resin to be used. Finally, a horizontal resolution of $4,21\mu m^2$ was obtained. Even so, when printing small squares, the edges were slightly bordered. This may be due to many reasons; bad focus, inadequate curing time, damaged coating material in the resin vat, etc.

The next step was to print simple parts to ensure correct operation of the linear actuator. First, we printed very simple pieces in which the only thing that varied was the number of layers. Then, we printed another series modifying the cross section and the geometry. The greatest number of problems appeared at this experimental part. On the one hand, it was necessary to adjust the speed of the stepper motor until no step was skipped. In addition, many problems related to the coating material, the inclination of the system and the required intensity in the LED appeared.

After analyzing the results obtained, the correct operation of the printer can be corroborated. However, there are future lines of work that would help to improve the current operation and obtain more complex pieces with better quality. As discussed above, in order to try to improve the horizontal resolution, simple tests can be developed to try to optimize the focus of the system as well as the curing time of the resin to be used. On the other hand, to try to improve the vertical resolution and to obtain pieces of great complexity, it would be interesting to optimize the resin by varying the concentration of photoinitiators and neutral absorbers to find the best suiting with the set-up created. In addition, trying to look for new coating materials would be needed, since in many occasions the main problem at the time of printing was the adhesion of the sample to the resin vat and not to the platform, reason why it was necessary to repeat the process several times until getting the desired sample. Finally, one of the most important lines of work would be the development of a device that allows a precise measurement of the distance between the platform and the resin vat, since at this moment this process is done intuitively and in case of using resins with a low depth of penetration, it is a very complicated task.

Currently, this technique presents great limitations, as it can be its low resolution, as well as the existence of very few suitable materials. As mentioned throughout the thesis, the resolution is affected by the software used, the optical system, resins, etc. So these are the parameters that need to be studied in depth in order to be able to improve this technique and expand its use.

References

- [1] I. Gibson, D. Rosen and B. Stucker, *Additive Manufacturing Technologies*, New York: Springer, 2010.
- [2] C. Hull, "Apparatus for Production of Three-Dimensional Objects by Stereolithography". Patent 4.575.330, 1986.
- [3] J. Andre, A. Le Mehaute and A. De Witte, "Dispositif pour realiser un modele de piece industrielle ("Dispositive for Constructing a Model of an Industrial Component)". France Patent 11241, 1984.
- [4] A. Gill, *Applications of Microstereolithography in Tissue Engineering*, Bachelor Thesis of Materials Science and Engineering: University Of Sheffield, 2012.
- [5] A. Bertsch, S. Jiguet, P. Bernhard and P. Renaud, "Microstereolithography: a Review," *MRS Proceedings*, vol. 758, 2002.
- [6] M. Berger, "Nanotechnology and 3D-printing," 2014. [Online]. Available: <http://nanoworker.com/spotlight/spotid=37541.php>. [Accessed 27 January 2017].
- [7] M. Lambert, A. Campaigne III and W. B., "Design Considerations for Mask Projection Microstereolithography Systems," 2013 [Online]. Available: <https://sffsymposium.engr.utexas.edu/Manuscripts/2013/2013-09-Lambert.pdf>. [Accessed 27 January 2017].
- [8] P. Lehtinen, *Projection Microstereolithography Equipment*, Master's Thesis: Aalto University School of Science, 2013.
- [9] S. Lee, H. Kang, J. Park, S. Rhie, S. Hahn and D. Cho, "Application of Microstereolithography in the Development of Three-Dimensional Cartilage Regeneration Scaffolds," *Biomedical Microdevices*, vol. 10, no. 2, pp. 233-241, 2007.
- [10] K. Mazey, "3. P. f. t. H. Impaired," 2017. [Online]. Available: <http://www.engineering.com/3DPrinting/3DPrintingArticles/ArticleID/5128/3D-Printing-For-the-Hearing-Impaired.aspx>. [Accessed 27 January 2017].
- [11] Y. Patril and R. Patril, "Improving Stereolithography Resolution," *International Journal of Modern Trends in Engineering and Research*, vol. 3, no.2349-9754 2016.
- [12] "DIY high resolution SLA/DLP printer building blog," 2013. [Online]. Available: http://www.khwellng.nl/3d.dlp_printer.php. [Accessed 28 January 2017].
- [13] E. Palermo, "What is Stereolithography?," 2016. [Online]. Available: <http://www.livescience.com/38190-stereolithography.html>. [Accessed 27 January 2017].
- [14] M. Tehfe, F. Louradour, J. Lalevée and J. Fouassier, "Photopolymerization Reactions: On the Way to a Green and Sustainable Chemistry," *Applied Science*, vol. 3, no. 2, pp. 490-514, 2013.
- [15] K. Ohno, M. Tanaka, J. Takeda and Y. Kawazoe, *Nano and Micromaterials*, Berlin: Springer, 2008.
- [16] S. Zissi, A. Bertsch, S. Corbel, J. Andro and D. Lougnot, "Microstereophotolithography using a liquid crystal display as dynamic mask-generator," *Microsystem Technologies* vol. 3, no. 2, pp. 42-47, 1996.

- [17] C. Zhou, H. Ye and F. Zhang, "A Novel Low-Cost Stereolithography Process Based on Vector Scanning and Mask Projection for High-Accuracy, High-Speed, High-Throughput, and Large-Area Fabrication," *Journal of Computing and Information Science in Engineering*, vol. 15, no. 1, pp. 011003-011003-8, 2015.
- [18] "Mask-Image-Projection-based Stereolithography," 2017. [Online]. Available: <http://www.craft-usc.com/technologies/mip-sl/>. [Accessed 25 January 2017].
- [19] M. Farasi, S. Huang, P. Birch, F. Claret-Tournier, R. Young, D. Budgett, C. Bradfield and C. Chatwin, "Microfabrication by use of a spatial light modulator in the ultraviolet: experimental results," *Optic Letters*, vol. 24, no. 8, p. 549, 1999.
- [20] J. Jackson, "Visual Analysis of a Texas Instruments Digital Micromirror Device," 2017. [Online]. Available: <http://www.optics.rochester.edu/workgroups/cml/opt307/spr05/john/>. [Accessed 27 January 2017].
- [21] C. Sun, N. Fang, D. Wu and X. Zhang, "Projection Microstereolithography using digital micromirror device," *Sensors and Actuators A: Physical*, vol. 121, no. 1, pp. 113-120, 2005.
- [22] "LCoS (Light Crystal over Silicon)" [Online]. Available: <http://www.tech-faq.com/lcos.html> [Accessed 28 January 2017].
- [23] X. Zheng, J. Deotte, M. Alonso, G. Farquar, T. Weisgraber, S. Germberling, H. Lee, N. Fang and C. Spadaccini, "Design and Optimization of a Light-emitting Diode Projection Micro-stereolithography Three-Dimensional Manufacturing System," *Review of scientific Instruments*, vol.84, 2012.
- [24] "Acerca de los faros de vehículos utilizando DMD," 2013. [Online]. Available: http://global-autonews.com/bbs/board.php?bo_table=bd_013&wr_id=575.
- [25] "Choosing a Collimation Lens for Your Laser Diode," [Online]. Available: <https://www.thorlabs.com/tutorials.cfm?tabID=f7ed0dd5-3f31-4f84-9843-e0f7ac33f413>. [Accessed 08 February 2017].
- [26] "AL3026-A - Ø30 mm S-LAH64 Aspheric Lens, f=26 mm, NA=0.51, ARC: 350-700 nm," [Online]. Available: <https://www.thorlabs.com/thorproduct.cfm?partnumber=AL3026-A..> [Accessed 08 February 2017].
- [27] "N10X-PF - 10X Nikon Plan Fluorite Imaging Objective, 0.3 NA, 16 mm WD" [Online]. Available: <https://www.thorlabs.com/thorproduct.cfm?partnumber=N10X-PF> [Accessed 08 February 2017].
- [28] "Bargaining -HIWIN linear guide module, KK4001P-100A1-F0 original factory more assured," [Online]. Available: <http://www.offerany.com/p-14812114866.html>. [Accessed 01 February 2017].
- [29] "catalog.orientalmotor.com," [Online]. Available: <http://catalog.orientalmotor.com/plp/itemdetail.aspx?cid=1002&categoryname=all-categories&productname=pk-series-stepping-motors&itemname=pk244pda-p10&cid=1002&prodid=3001048&itemid=36182&backtoname=Item+%23+RBD228A-K&pane=sb&bc=100%7C3001063x&isUOM=1>. [Accessed 01 February 2017].
- [30] *Creation Workshop. Envision Labs.*
- [31] Y. Pan, C. Zhou and Y. Chen, "Rapid Manufacturing in Minutes: The Development of a Mask Projection," *International Manufacturing Science and Engineering Conferences*, no. MSEC2012-7232, pp. 405-414, 2012.

- [32] " CLIP: The New Game-Changing Layerless 3D Printing Technology," [Online]. Available: <http://www.designorate.com/wp-content/uploads/2015/07/carbon-3d-clip-printing.jpg>. [Accessed 12 May 2017].
- [33] "Continious Liquid Interface Production," 2015. [Online]. Available: <https://www.3dprintwise.com/wp-content/uploads/2015/05/carbon-3d.jpg>. [Accessed 12 May 2017].
- [34] J. Deena and T. Kochunni, "Difference Between Light Microscope and Electron Microscope," [Online]. Available: <http://www.biologyexams4u.com/2012/10/difference-between-light-microscope-and.html#.WJl-KfmLRPY>. [Accessed: 07 February 2017]
- [35] T. Palucka, "History of the Electron Microscope, 1931-2000," 2002. [Online]. Available: http://authors.library.caltech.edu/5456/1/hrst.mit.edu/hrs/materials/public/ElectronMicroscope/EM_HistOverview.htm.. [Accessed 08 February 2017].
- [36] "How Microscopes Work," [Online]. Available: <http://isbbio1.pbworks.com/w/page/9205983/Group%205>. [Accessed 07 February 2017].
- [37] J. Atteberry, "H. S. M. E. Work," 2009 [Online]. Available: <http://science.howstuffworks.com/scanning-electron-microscope2.htm>. [Accessed 07 February 2017].

Appendix 1

The next table shows the budget expended during this Master's Thesis without considering VAT:

Table 7. Master's Thesis budget

Product	Units	Price (Euros/unit)	Total price (Euros)
Light source	1	15,80	15,80
Light source mounting	1	24,20	24,20
Lens mounting	2	26,00	52,00
Collimating lenses	2	272,00	544,00
Aperture	1	51,25	51,25
Post	12	5,28	63,36
Right angle post clamp	4	8,78	35,12
Swivel angle post clamp	1	20,34	20,34
Post anchors	3	23,97	71,91
Pedestal pillar posts	3	27,50	82,50
Aluminum breadboard anchors	1	27,00	27,00
Aluminum breadboards	1	116,00	116,00
Aluminum breadboards	1	165,00	165,00
Mirror	1	46,50	46,50
Mirror mounting	1	14,50	14,50
Screws	1	7,00	7,00
Step stepper motor	1	304,00	304,00
Linear actuator	1	498,00	498,00
Coupler	1	50,45	50,45
Microscope	1	767,00	767,00
Power source	1	20,00	20,00
Arduino	1	50,00	50,00
Aluminum Breadboard	1	44,50	44,50
Large Right-Angle Bracket, M6 Holes	1	149,00	149,00
Post anchors	4	25,13	100,52
Post	2	4,47	8,94
Total			3328,89